

ACCEPTED MANUSCRIPT • OPEN ACCESS

Between life and death: strategies to reduce phototoxicity in super-resolution microscopy

To cite this article before publication: Kalina L. Tosheva *et al* 2020 *J. Phys. D: Appl. Phys.* in press <https://doi.org/10.1088/1361-6463/ab6b95>

Manuscript version: Accepted Manuscript

Accepted Manuscript is “the version of the article accepted for publication including all changes made as a result of the peer review process, and which may also include the addition to the article by IOP Publishing of a header, an article ID, a cover sheet and/or an ‘Accepted Manuscript’ watermark, but excluding any other editing, typesetting or other changes made by IOP Publishing and/or its licensors”

This Accepted Manuscript is © 2020 IOP Publishing Ltd.

As the Version of Record of this article is going to be / has been published on a gold open access basis under a CC BY 3.0 licence, this Accepted Manuscript is available for reuse under a CC BY 3.0 licence immediately.

Everyone is permitted to use all or part of the original content in this article, provided that they adhere to all the terms of the licence <https://creativecommons.org/licenses/by/3.0>

Although reasonable endeavours have been taken to obtain all necessary permissions from third parties to include their copyrighted content within this article, their full citation and copyright line may not be present in this Accepted Manuscript version. Before using any content from this article, please refer to the Version of Record on IOPscience once published for full citation and copyright details, as permissions may be required. All third party content is fully copyright protected and is not published on a gold open access basis under a CC BY licence, unless that is specifically stated in the figure caption in the Version of Record.

View the [article online](#) for updates and enhancements.

Between life and death: strategies to reduce phototoxicity in Super-Resolution Microscopy

Kalina L. Tosheva¹, Yue Yuan¹, Pedro Matos Pereira², Siân Culley^{1,3}, and Ricardo Henriques^{1,3}

¹MRC Laboratory for Molecular Cell Biology, University College London, London, UK

²ITQB-NOVA, Oeiras, Portugal

³The Francis Crick Institute, London, UK

Super-Resolution Microscopy enables non-invasive, molecule-specific imaging of the internal structure and dynamics of cells with sub-diffraction limit spatial resolution. One of its major limitations is the requirement for high-intensity illumination, generating considerable cellular phototoxicity. This factor considerably limits the capacity for live-cell observations, particularly for extended periods of time. Here, we give an overview of new developments in hardware, software and probe chemistry aiming to reduce phototoxicity. Additionally, we discuss how the choice of biological model and sample environment impacts the capacity for live-cell observations.

Phototoxicity | Photodamage | Super-Resolution Microscopy | Fluorescence

Correspondence: s.culley@ucl.ac.uk, r.henriques@ucl.ac.uk

19 Introduction

20 The spatial resolution of an imaging system is
21 defined as the capacity to distinguish closely
22 separated features; in light microscopy, this is
23 limited by diffraction to ~ 200-300 nm

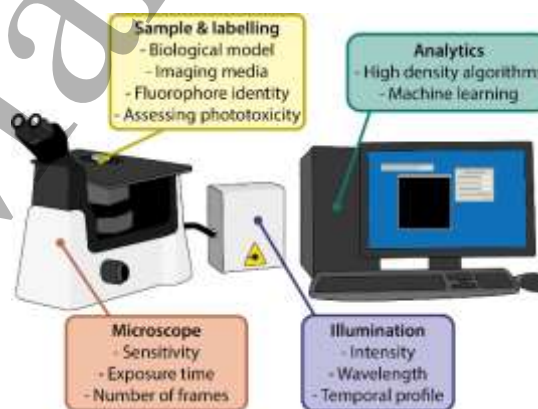
24 . Consequently, microscopy approaches developed
25 to achieve resolutions beyond this limit are termed
26 'Super-Resolution Microscopy' (SRM) [1]. SRM
27 techniques that have recently gained popularity,
28 such as Photoactivated Localisation Microscopy
29 (PALM) [2], Stochastic Optical Reconstruction
30 Microscopy (STORM) [3], Structured Illumination
31 Microscopy (SIM) [4] and Stimulated Emission
32 Depletion (STED) Microscopy [5], have enabled
33 biological discoveries inaccessible to conventional
34 microscopy [6]–[9]. Alongside increased spatial

35 resolution, SRM retains many desirable features of
36 light microscopy techniques, including molecule-
37 specific labelling and the potential for live-cell
38 imaging, unavailable to other high-resolution
39 techniques, such as electron microscopy. However,
40 the live-cell imaging potential of SRM has remained

41 largely untapped as the requirements of most SRM
42 techniques pose various challenges for exploring
43 dynamic processes under physiological conditions.
44 In contrast, such limitations are absent when using
45 fixed specimens.

46 Resolution increase in SRM is generally achieved at
47 the cost of high-intensity illumination [10]. These
48 requirements result in photobleaching, defined as
49 irreversible loss of fluorescence during imaging.
50 However, of greater importance to live-cell imaging
51 is sample health. Thereby, the dependency of SRM
52 on illumination intensities orders of magnitude

53 higher than conventional microscopy (W/cm^2 -
54 GW/cm^2 compared to mW/cm^2 - W/cm^2) makes
55 phototoxicity the biggest concern when employing
56 these techniques [10], [11]. In the context of
57 microscopy, phototoxicity is a broad term
58 encompassing physical and chemical reactions
59 caused by the interaction between light and cellular
60 components, with detrimental effects on the latter
61 [12], [13]. Correct biological interpretations from live-
62 cell imaging can only be achieved if the observed
63 phenomena progress with minimal perturbation [14].
64 A multitude of properties of the sample and the
65 imaging can influence phototoxicity and can thus be
66 optimised for improving SRM for live-cell imaging
67 (Fig. 1).

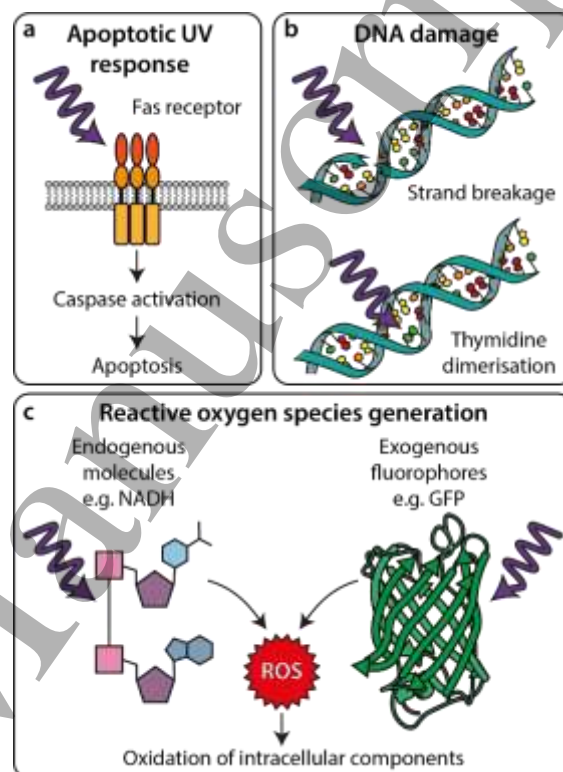


68
69 **Fig. 1 Summary of the factors that can be optimised to reduce**
70 **phototoxicity in Super-Resolution Microscopy.**

71 On a molecular level, the main causes of
72 phototoxicity are photochemical processes that
73 directly damage intracellular components or lead to
74 the production of toxic products within the cell or in
75 its direct environment [15], [16]. The detrimental
76 effects of ultraviolet (UV) light on cells is particularly
77 well characterised; illumination with UV light can
78 trigger the so-called 'UV-response' (Fig. 2) Fig. 1
79 Summary of the factors that can be optimised to reduce
80 phototoxicity in Super-Resolution Microscopy.) [17], [18],

81 DNA-strand breaks [19], [20], and thymidine
 82 dimerisations [21] (**Fig. 2b**Fig. 1 Summary of the factors
 83 that can be optimised to reduce phototoxicity in Super-
 84 Resolution Microscopy.), leading to mutations and
 85 downstream apoptosis [22], [23]. Additionally, both
 86 UV and visible wavelengths can excite other
 87 endogenous photoactive molecules in the cell, such
 88 as NAD(P)H [24], flavins [25], [26] and
 89 porphyrins[27], [28]. Furthermore, in fluorescence
 90 microscopy there are phototoxic effects associated
 91 with the fluorescent molecules required for labelling
 92 structures [15], [29]. Upon illumination, both
 93 endogenous and exogenous photoactive molecules
 94 can be excited to reactive states (most commonly
 95 long-lived triplet states) capable of undergoing redox
 96 reactions that lead to formation of reactive oxygen
 97 species (ROS) (**Fig. 2c**Fig. 1 Summary of the factors that
 98 can be optimised to reduce phototoxicity in Super-Resolution
 99 Microscopy.). ROS are considered the major
 100 contributors to phototoxicity [12], [13]. Their
 101 production can occur via direct reaction between the
 102 excited molecule and environmental molecular
 103 oxygen or via reactions with other neighbouring
 104 molecules that generate free radicals [30]. ROS
 105 have a broad range of negative effects ranging from
 106 oxidising proteins, lipids, and DNA, as well as
 107 systematic effects such as disrupting the redox
 108 homeostasis, signalling pathways and cell cycle
 109 [12], [31]. Notably, ROS production correlates with
 110 illumination intensity and photobleaching [12], [15],
 111 both of which are issues present in SRM. As a result,
 112 there is considerable interest in developing SRM
 113 technologies for improved sample health. Here, we
 114 will outline the progress in hardware, software and

115 probe development as well as choices in biological
 116 model and sample preparation that can help
 117 improve live-cell SRM (**Fig. 1**)
 118 **Quantifying phototoxicity in microscopy**
 119 Measuring phototoxicity in microscopy is not a trivial
 120 problem, as evidenced by the sparsity of the



121
 122 **Fig. 2 Interactions of light with cellular components leading to**
 123 **phototoxicity. a** UV light can trigger apoptosis by inducing Fas
 124 receptor-mediated signalling pathways. **b** UV light can directly
 125 damage DNA by causing strand breakage (top) or thymidine
 126 dimerisation (bottom), causing mutations and inducing DNA
 127 damage responses. **c** UV and visible wavelengths can excite
 128 photoactive molecules leading to chemical generation of ROS,
 129 which can then damage cellular components.

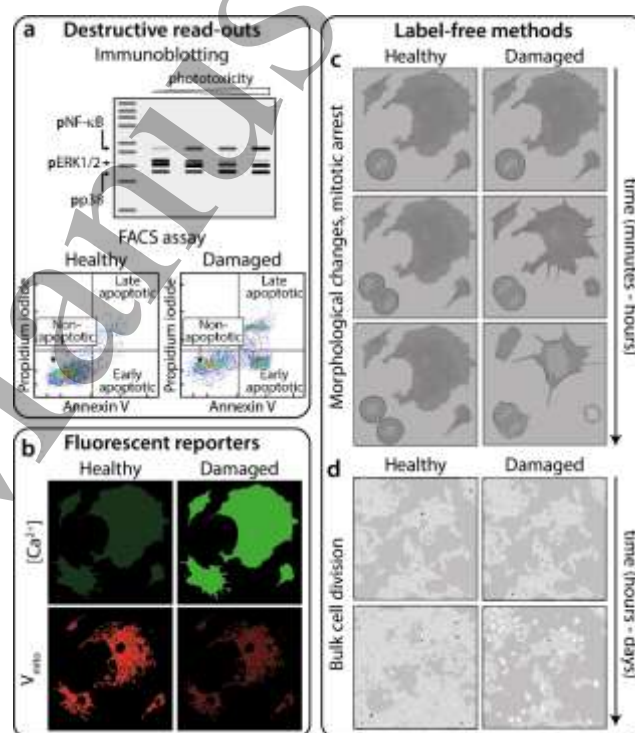
130 available literature [12], [13]. This is not entirely
 131 surprising, as phototoxicity is mediated by many
 132 factors (**Fig. 1**). These include illumination
 133 wavelength, intensity and duration of illumination,
 134 the illumination regime (e.g. LED illumination vs.
 135 laser illumination, laser-scanning vs. light-sheet),
 136 and the number of imaged 3D-planes [32]–[37].
 137 Additionally, illumination tolerance can vary
 138 substantially between specimens (see Biological

139 models and sample preparation section), and
 140 experimental stress can influence a specimen's
 141 sensitivity to illumination [14]. For example, a
 142 procedure as routine as transfection or the addition
 143 of a drug has been shown to dramatically increase
 144 cellular sensitivity to light [10], [38]. Therefore, steps
 145 must be taken to reduce avoidable experimental
 146 perturbations which can influence the well-being of
 147 the sample in an illumination-independent manner,
 148 e. g. suboptimal environmental conditions
 149 (temperature, pH, etc.) [39] or complex sample
 150 mounting.

151 How does one approach a problem as versatile as
 152 measuring phototoxicity? An intuitive and common
 153 way of assessing photodamage is by measuring
 154 photobleaching [40]–[43]. However, phototoxicity
 155 and photobleaching are two separate processes;
 156 while toxic ROS are produced during
 157 photobleaching, they can also be generated
 158 independently of this process [15], [44]. Therefore,
 159 phototoxicity can commence prior to a detectable
 160 reduction in fluorescence, making photobleaching
 161 an unreliable read-out for photodamage in the
 162 context of live-cell imaging [12]. More importantly,
 163 photobleaching rates give no information on the
 164 health and viability of the specimen. Thus, a better
 165 phototoxicity measure would have a read-out related
 166 to the properties of the sample itself, rather than the
 167 properties of the fluorescence [34].

168 There are several *in vitro* assays for post-imaging
 169 assessment of the health and viability of a specimen
 170 that can be used to indicate whether phototoxicity
 171 occurred (Fig. 3a). These include detection of toxic
 172 ROS, fragmentation and oxidation of DNA strands,

173 reduced metabolic activity, loss of membrane
 174 integrity and the expression of stress- and
 175 apoptosis-related proteins [45]–[50]. The
 176 advantages are that these assays provide an
 177 inexpensive and simple specimen viability
 178 evaluation. Thus, different illumination conditions
 179 can be tested and viability can be assessed each
 180 time. However, for such assays the measurement is
 181 limited to a single timepoint and imaging cannot be
 182 recommended after performing the assay.



183

184 **Fig. 3 Methods for measuring phototoxicity.** a 'Destructive
 185 read-outs' are techniques prohibiting further imaging of the
 186 sample. These include blotting for phosphorylated forms of
 187 proteins present in damage-activated pathways [51] and flow
 188 cytometry for determining the population of cells expressing,
 189 for example, apoptotic markers such as annexin V. b
 190 'Fluorescent reporters' are additional indicators added to the
 191 sample during imaging whose fluorescence signal changes in
 192 response to e.g. intracellular Ca^{2+} concentration (top) or
 193 mitochondrial membrane potential (bottom). 'Label-free
 194 methods' of quantifying phototoxicity involve: c short-term
 195 observation of cell division and morphology and d proliferation
 196 of cells in culture following imaging.

197 A more dynamic and practical approach entails
 198 monitoring changes in relevant biological
 199 parameters during imaging (Fig. 3b, c). Cellular

1
2
3 200 processes which are particularly photosensitive (i.e.
4 201 rapidly perturbed by light) are excellent read-outs.
5 202 For example, a commonly employed method is
6 203 measuring changes in cytosolic calcium
7 204 concentration using calcium-sensitive fluorescent
8 205 probes [50], [52]–[54] (**Fig. 3b**, top). This strategy
9 206 was used to evaluate live-cell STED microscopy by
10 207 monitoring differences in intracellular calcium
11 208 concentration between control cells and STED-
12 209 imaged cells. This method showed that while there
13 210 is little difference between calcium concentration in
14 211 control and STED-imaged cells when using
15 212 excitation and STED-lasers with wavelengths >600
16 213 nm, responses indicative of cell damage were
17 214 observed with shorter illumination wavelengths and
18 215 when longer STED-laser dwell times were used [29].
19 216 Other processes exist that make suitable read-outs
20 217 for phototoxicity, including changes in mitochondrial
21 218 membrane potential [41], [51] (**Fig. 3b**, bottom),
22 219 reduction of chromosome movement [55] and
23 220 slowing of microtubule growth [10]. It is worth
24 221 highlighting that, regardless of the process chosen,
25 222 care must be taken when employing fluorescent
26 223 probes for visualising these read-outs [46], [56].
27 224 There are image-based phototoxicity
28 225 measurements that can be performed without
29 226 fluorescent labels. These often rely on identifying
30 227 changes in cell morphology indicative of entry into
31 228 apoptosis, such as blebbing or cell rounding [10],
32 229 [14], [51], [57], for example by using transmitted light
33 230 imaging (**Fig. 3c**). This approach was recently used
34 231 to train a deep convolutional neural network,
35 232 referred to as 'DeadNet', with the objective to
36 233 automate phototoxicity detection and quantification

234 from transmitted light images [58]. However, despite
235 widespread use, relying on morphology as a read-
236 out has two limitations: first, even experienced
237 researchers can struggle to identify subtle changes
238 in morphology, thus biasing the results (e.g. by
239 annotating ambiguous cases incorrectly [58];
240 second, when changes become obvious, they
241 usually represent an extreme phenotype indicative
242 of irreversible damage. Thus, they cannot account
243 for early damage that may arise even as cells
244 display a healthy morphology [13], [39].
245 In this context, a read-out that deserves special
246 mention is cell division (**Fig. 3c, d**): a well-
247 characterised biological process with easily
248 identifiable phases. It is highly regulated and
249 sensitive to various perturbations, including
250 illumination and changes in ROS concentrations
251 [15], [31]. This makes cell cycle an excellent read-
252 out for detection and quantification of phototoxicity
253 [39], with both continuous (**Fig. 3c**) and endpoint
254 (**Fig. 3d**) measurements possible. Delay in mitotic
255 progression has been used successfully to detect
256 perturbations in the health of both cultured cells and
257 developing embryos [32]–[35]. Additionally,
258 evaluating colony formation or number of cell
259 divisions after illumination (typically assessed after
260 a period of one or more cell cycles) can be indicative
261 of long-lasting damage [12], [29] (**Fig. 3d**). This
262 approach was used to perform extensive
263 characterisation of photodamage under illumination
264 conditions commonly used in single-molecule
265 localisation microscopy (SMLM) [10]. The viability of
266 several different cell lines was determined 20–24 h
267 post illumination, a strong correlation between

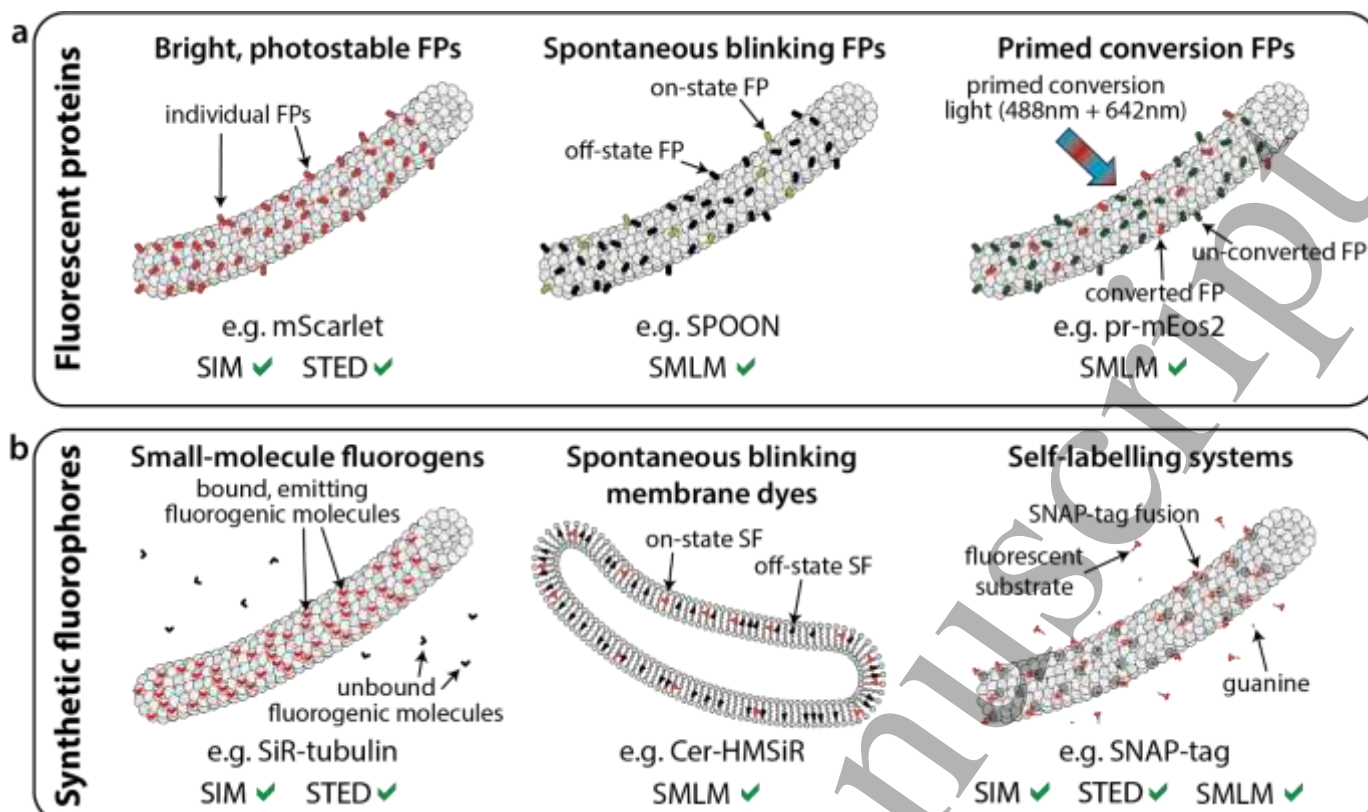


Fig. 4 Low phototoxicity fluorescent probes and labelling for live-cell Super-Resolution Microscopy. Various recently-developed fluorescent protein- (a) and synthetic fluorophore- (b) based methods for labelling in live-cell super-resolution. All labels are shown attached to a microtubule as an example of an intracellular structure, with the exception of the Cer-HMSiR membrane dye in b.

268 shorter illumination wavelengths and increased cell
 269 death was shown, particularly at high intensities.
 270 However, results also suggested that long-term cell
 271 viability is possible even with illumination
 272 wavelengths as short as 405 nm, provided the
 273 integrated light dose is small, preferably with
 274 continuous rather than pulsed illumination.
 275 Naturally, a limitation exists in employing these
 276 methods to assess phototoxicity in post-mitotic
 277 systems, e.g. primary neuron cultures. However, for
 278 relevant models, choosing mitosis as a read-out has
 279 the significant advantage of allowing phototoxicity
 280 assessment based on label-free transmitted light
 281 images [10], [29], [33], minimising the introducing
 282 additional damage during evaluation.
 283 From reports of phototoxicity in literature, several
 284 conclusions can be drawn to guide live-cell friendly

285 SRM. Firstly, red-shifted wavelengths are preferable
 286 to shorter wavelengths. In particular, UV
 287 wavelengths should be avoided wherever possible
 288 [10], [29], [33]. Furthermore, several studies
 289 demonstrate that lower intensity illumination with
 290 longer exposure is less damaging than short intense
 291 bursts or pulses of illumination [10], [34], [40]. Most
 292 importantly, a recurrent message throughout the
 293 literature is that higher illumination intensities are
 294 more damaging than corresponding imaging
 295 conditions with lower illumination intensities. We
 296 anticipate that real-time phototoxicity
 297 measurements will become commonplace in both
 298 diffraction-limited microscopy and SRM, and that
 299 future SRM techniques will be accompanied by a
 300 thorough description of how they impact living

301 samples. Concomitantly, for SRM users, awareness
302 of strategies for minimising phototoxicity is crucial.

303 **Fluorescent probe development for live-cell** 304 **Super-Resolution Microscopy**

305 SRM techniques have distinct requirements for
306 fluorescent probes. SIM quality relies on collecting
307 images of high Signal-to-Noise Ratio (SNR),
308 generally achieved by labelling with fluorophores of
309 high brightness and resistance to photobleaching. In
310 STED, fluorophores must not only be bright but also
311 possess a large Stokes-shift and stimulated
312 emission cross-section at the STED wavelength
313 [59]. SMLM techniques have the most demanding
314 labelling requirements - fluorophores must be
315 capable of cycling between 'on' and 'off' states with
316 appropriate kinetics, a high quantum yield in the on-
317 state, and a very low quantum yield in the off-state.
318 Several fluorophores and probes have been
319 developed specifically for SRM [60], [61]. However,
320 while many specialised fluorophores exist for fixed
321 specimens [62], there are far fewer options available
322 for live-cell imaging. An inappropriate choice of
323 fluorophore for live-cell SRM will not only lead to low
324 quality images downstream [63], but also inevitably
325 impact acquisition settings and hence phototoxicity
326 [10], [64].

327 As for most fluorescence microscopy techniques,
328 the two classes of fluorophores used in SRM are
329 fluorescent proteins (FPs) (**Fig. 4a**) and synthetic
330 fluorophores (SFs) (**Fig. 4b**). FPs are the usual
331 choice for live-cell imaging as they can be fused to
332 a target of interest via genetic encoding, but at the
333 cost of reduced brightness compared to SFs. The

334 recent development of bright and photobleaching-
335 resistant FPs has expanded the options for SIM and
336 STED (**Fig. 4a**, left). Examples of these new FPs are
337 mNeonGreen ($\lambda_{\text{ex}}=506$ nm) [65], mScarlet
338 ($\lambda_{\text{ex}}=569$ nm) [66] and mGarnet ($\lambda_{\text{ex}}=598$ nm) [67].
339 SMLM techniques generally require
340 photoswitchable fluorophores (e.g. mEos3.2,
341 rsKame) [68], [69]. Despite the availability of several
342 photoswitchable FPs, their use in live-cell imaging
343 remains challenging [10], [64]. The chief reason is
344 that transitions between off- and on-states are
345 typically modulated by UV illumination. The
346 combination of this with high intensity excitation for
347 detection of molecular positions results in a short
348 window for live-cell SMLM studies. To reduce
349 phototoxicity in SMLM, FPs that do not require UV
350 pumping for photoswitching are being developed
351 (**Fig. 4a**, centre), with one such example being
352 SPOON [70]. Primed conversion is another
353 promising UV-independent approach to induce
354 photoswitching (**Fig. 4a**, right) [71]. Thereby a
355 combination of blue and near-infrared illumination
356 induces photoconversion in Dendra2 and the newly
357 developed primed-conversion protein pr-mEos2
358 [71], [72]. Recently, a general mechanism for primed
359 conversion was described, which is anticipated to
360 accelerate the development of more FPs that can be
361 photoconverted with this live-cell friendly approach
362 [73]. FPs for other specific SRM techniques have
363 also been developed (e.g. SkyIan-NS for non-linear
364 SIM or GMars for REversible Saturable/switchable
365 Optical Fluorescence Transitions, RESOLFT) [74],
366 [75].

1
2
3 367 The second alternative, SFs (**Fig. 4b**), are small
4
5 368 chemically synthesised probes. These have higher
6
7 369 quantum yields and are more robust against
8
9 370 photobleaching than FPs [76]–[79]. While there are
10
11 371 some cell-permeable SFs that can be used to label
12
13 372 specific proteins (e.g. fluorogens such as SiR-
14
15 373 tubulin and SiR-actin) (**Fig. 4b**, left) [80], [81] or cell
16
17 374 compartments directly (e.g. Membright, ER-Tracker
18
19 375 or MitoTracker) (**Fig. 4b**, centre) [77], [82]–[84],
20
21 376 additional 'linker' molecules are normally required to
22
23 377 associate SFs with the structure of interest. These
24
25 378 linkers must bind the target structure with high
26
27 379 affinity and specificity (e.g. antibodies and
28
29 380 DNA/RNA scaffolds, usually using amine- or thiol-
30
31 381 reactive derivatives of the SF) [85]. However, many
32
33 382 of these high-affinity linkers and SFs are not cell-
34
35 383 permeable, which limits their use in live-cell SRM to
36
37 384 labelling of cell-surface molecules. If genetic
38
39 385 encoding is possible and preferable, cell-permeable
40
41 386 SFs can be combined with flexible self-labelling
42
43 387 systems, such as SNAP-tag, Halo-tag or FIAsH (**Fig.**
44
45 388 **4b**, right) [86]–[89]. An elegant example of such an
46
47 389 approach is the use of Cox8A-SNAP fusion labelled
48
49 390 with SNAP-Cell SiR for STED. This has enabled the
50
51 391 visualisation of the dynamics of mitochondrial
52
53 392 cristae with ~70 nm resolution [90].
54
55 393 SFs have also been engineered for live-cell SRM.
56
57 394 Spontaneously blinking synthetic fluorophores (e.g.
58
59 395 HMSiR) have been recently developed (**Fig. 4b**,
60
396 center). They do not require UV irradiation or
397 cytotoxic additives (such as thiol) to induce
398 photoswitching [91], [92]. High photostability SFs

399 have also been developed, enabling live-cell STED
400 [79], [93]–[95].

401 A final regime for live-cell SRM-compatible labelling
402 is based on site-specific conjugation of fluorophores
403 to a target of interest, through genetic code
404 modifications and click chemistry (**Fig. 4b**, right)
405 [96]–[98]. These approaches combine the benefits
406 of site-specific labelling (as is the case for FPs) with
407 no requirement for protein expression and bright
408 labels (as is the case for SFs).

409

410 **Biological models and sample preparation**

411 Care should be taken when selecting a biological
412 model for SRM. Cellular sensitivity to light exposure
413 can vary based on cell type and species [10], [14],
414 [45], and in the case of whole organisms,
415 developmental stage [13], [34]. Phototoxicity has
416 been documented for different cell types, ranging
417 from primary cells [13], [45] to various immortalised
418 cell lines [10], [26], [38], [99]. One such study
419 focuses on immortalised cell lines, where it shows
420 that COS-7 and U2OS cells exhibit similar
421 photosensitivity, whereas HeLa cells are
422 substantially more robust, potentially making the
423 latter a more suitable system for live-cell SRM
424 studies [10]. Another study illustrated the effect of
425 photodamage on primary cells from rat central
426 nervous system [45]. Here, illumination with blue
427 light could induce morphological changes,
428 differentiation or cell death depending on the cell
429 type.

430 When imaging whole organisms, earlier
431 developmental stages from the same species tend
432 to be more photosensitive than later [12].

1
2
3 433 Furthermore, different model organisms display 467 the medium, thus minimising photobleaching and
4 434 variable photosensitivity. For example, fruit fly 468 phototoxicity [105], [106]. While these approaches
5 435 embryos and nematode worms have higher 469 could improve live-cell SRM, it should be noted that
6 436 illumination tolerances than zebrafish embryos, 470 they are only suitable for specimens which can
7 437 corals or cultured cells [13], [14]. Even within the 471 tolerate hypoxia or anoxia. Notably, some
8 438 same cell, different intracellular structures exhibit 472 fluorophores used in SRM require oxygen
9 439 different responses to illumination [29], [100]. 473 scavenger systems to photoswitch, however, these
10 440 Photodamage can be mitigated through additional 474 buffers typically use cytotoxic compounds such as
11 441 sample preparation steps. Established strategies 475 thiols, making them unsuitable for live-cell imaging.
12 442 centre on preventing photobleaching by modifying 476 A different strategy for reduction of ROS during
13 443 the sample environment. As photobleaching can 477 imaging involves supplementing the media with
14 444 contribute to phototoxicity via ROS production [44], 478 antioxidants. Antioxidants are molecules that
15 445 strategies to reduce photobleaching could also help 479 prevent oxidation in a biological context [107].
16 446 ameliorate phototoxicity [15], [29], [101]. One 480 Among antioxidants, Trolox, the soluble form of
17 447 strategy is to modify the environmental conditions 481 vitamin E, has been shown to have a protective
18 448 prior to or during imaging. A prime example is 482 effect for a number of cell lines due to its ROS-
19 449 removal of oxygen, the main effector of 483 neutralising properties [108]. The presence of the
20 450 photobleaching [102], from the culture medium. This 484 antioxidant in the sample medium has been shown
21 451 can be achieved by bubbling nitrogen through the 485 to increase the number of post-illumination mitotic
22 452 medium during imaging. This yields an increased 486 cells by up to 38% compared to cells illuminated
23 453 photostability [103], [104] and, since oxygen is 487 without Trolox [33]. However, this molecule is not
24 454 directly involved in the production of ROS, also 488 suitable for SMLM, as it has been shown to inhibit
25 455 reduces light-dependent oxidative stress on the 489 fluorophore blinking [109]. Another antioxidant used
26 456 sample. It has also been shown that growing cells in 490 in microscopy is rutin, a plant flavonoid shown to
27 457 a hypoxic environment (3% oxygen) yielded a 25% 491 reduce EGFP reddening [110], [111], although no
28 458 increase in mitosis entry after blue light irradiation 492 direct reduction of phototoxicity was demonstrated.
29 459 [33]. Other approaches to reduce oxygen in the 493 A notable example of a medium additive for live-cell
30 460 medium involve the addition of commercially 494 imaging is the vitamin- and antioxidant-rich
31 461 available oxygen-scavengers such as the Oxyrase® 495 'Supplements for Optogenetic Survival' (SOS). SOS
32 462 enzyme complex (developed by Oxyrase, Inc., 496 has been shown to increase viability and reduce
33 463 Mansfield, Ohio). In combination with suitable 497 photodamage in several cell types of the rat central
34 464 substrates, such as D/L-lactate or D/L-succinate, 498 nervous system [45].
35 465 these enzymes catalytically reduce the 499 There are chemicals used in mounting media, such
36 466 concentration of oxygen and free radicals present in 500 as various antioxidants, triplet-state quenchers and

1
2
3 501 radical scavengers, that can be used for
4 502 photobleaching reduction and ROS neutralisation.
5
6 503 These include ascorbic acid [112], n-propyl gallate
7
8 504 [112]–[114], p-phenylenediamine [114]–[116], 1,4-
9
10 505 diazobicyclo(2,2,2)-octane (DABCO) [114], [117],
11
12 506 mercaptoethylamine (MEA) and cyclooctatetraene
13
14 507 (COT) [112]. Their presence in mounting media for
15
16 508 reduction of photobleaching is well characterised
17
18 509 [112], [115], [118], however there is no
19
20 510 comprehensive study on the use of these chemicals
21
22 511 in live-cell imaging. As a result, there is little
23
24 512 information regarding biocompatible working
25
26 513 concentrations or biological side effects. Therefore,
27
28 514 while potentially useful, they require further
29
30 515 exploration prior to use in live-cell SRM.
31
32 516 Some substances commonly used as supplements
33
34 517 are known also to cause phototoxicity, such as
35
36 518 molecules with benzene rings which are intrinsically
37
38 519 fluorescent [111]. For example, common cell media
39
40 520 components, such as riboflavin and pyridoxal, can
41
42 521 enhance oxidative reddening of GFPs; this effect
43
44 522 accounts for a considerable part of GFP
45
46 523 photobleaching [119]. Depleting these substances
47
48 524 increases GFP photostability, indirectly reducing
49
50 525 photodamage [110]. Additionally, the combination of
51
52 526 riboflavin and tryptophan in media generates ROS
53
54 527 and induces cytotoxicity upon illumination, whereas
55
56 528 their removal alleviates this effect [120], [121].
57
58 529 Finally, the study that established the SOS
59
60 530 supplement [45] used it in combination with the
531 photoinert media NEUMO and MEMO, which also
532 lack riboflavin. These media were specifically
533 developed to prevent phototoxicity of nervous
534 system cells. A confounding example is 4-(2-

535 hydroxyethyl)-1-piperazineethanesulfonic acid
536 (HEPES), commonly used as a replacement for
537 carbon dioxide buffering during imaging [39].
538 However, early reports demonstrated that HEPES-
539 buffered media exposed to low-intensity white light
540 can generate toxic hydrogen peroxide with
541 detrimental effects on thymocyte or T-cell culture
542 [122], [123].
543 There is still a lack of information on SRM sample
544 preparation reducing phototoxicity. Many principles
545 can be transferred from conventional fluorescence
546 imaging. These include assessing photosensitivity
547 of the biological model, environmental conditions,
548 and attention to media composition.

549 **Hardware developments for improved live-** 550 **cell imaging**

551 The microscope configuration has a substantial
552 impact on the amount of photodamage experienced
553 by a specimen. **Fig. 5a** shows the common
554 illumination regimes for conventional microscopy
555 and SRM (widefield for SIM and SMLM, confocal for
556 STED). Basic optimisations of the microscope body,
557 for example minimising photon loss in the detection
558 path by using high-quality filters and sensitive
559 detectors, will reduce the illumination burden to
560 achieve suitable SNR [101]. In SRM approaches,
561 microscopes are built with high-quality components,
562 often having bespoke solutions to maximize signal
563 detection [124], [125]. In addition, the ever-present
564 phototoxic high-intensity illumination requirements
565 of most SRM techniques can be further ameliorated
566 using dedicated hardware designs. Interestingly, a
567 recent study shown low-illumination live-cell SRM

568 immediately followed by *in situ* fixation of the sample
 569 and high-illumination SRM [126]. This approach
 570 combines the collection of temporal information in
 571 living-cells with a mild resolution increase, then
 572 capture of higher resolution for a specific timepoint
 573 upon fixation.

589 leads to decreased photobleaching [127]. Similarly
 590 to confocal microscopy, scanning at a higher rate in
 591 STED has been shown to reduce photobleaching
 592 [42]; this is enabled by using fast resonant scanning
 593 mirrors rather than slower galvanometer scanning
 594 mirrors to scan the beam pair through the sample.

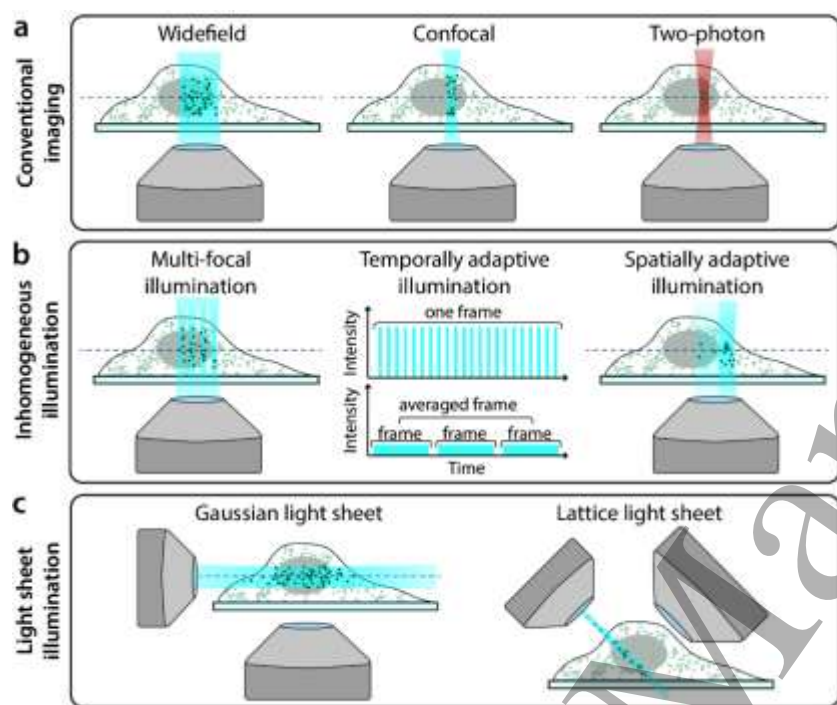


Fig. 5 Hardware modalities for conventional and low-phototoxicity Super-Resolution Microscopy. a Microscopy illumination regimes for conventional fluorescence imaging. **b** Examples of regimes that reduce light dose to the sample by inhomogeneous illumination. **c** Examples of light-sheet microscopy geometries.

574 In the case of STED, the presence of a second high-
 575 intensity laser beam (depletion laser) in addition to a
 576 confocal excitation beam confers the high
 577 phototoxicity of this method. However, the
 578 properties of both beams can have a substantial
 579 impact on sample photodamage. It has been shown
 580 in confocal microscopy that nanosecond pulsed,
 581 rather than continuous, excitation can reduce
 582 photobleaching, and that averaging multiple fast
 583 scans is less phototoxic than acquiring a single slow
 584 scan (**Fig. 5b**, 'Temporally adaptive illumination')
 585 [41]. The properties of the excitation beam have also
 586 been explored specifically in STED. For example,
 587 reducing the pulsing rate of the excitation laser
 588 allows time for long-lived triplet states to relax which

595 Another method described reducing phototoxicity in
 596 STED is by using two-photon excitation (**Fig. 5a**
 597 'Two-photon'). As two-photon excitation only excites
 598 fluorophores within the focal volume of the beam
 599 (rather than along the entire beam path, as is the
 600 case in single-photon excitation), it is often
 601 considered a more live-cell friendly imaging regime
 602 [54], [128]. Indeed, live-cell STED has been
 603 successfully demonstrated with two-photon
 604 excitation [129], [130] although while the former
 605 paper claims that there is no photodamage to the
 606 sample, this is not quantified. It should be noted that
 607 two-photon excitation does however increase local
 608 heating, which can damage the sample in a non-
 609 fluorophore mediated manner [131].

1
2
3 610 In STED microscopy with pulsed depletion lasers,
4
5 611 resolution scales non-linearly with beam intensity.
6
7 612 Thus, in order to obtain high resolution images, very
8
9 613 high (and phototoxic) depletion beam intensities are
10
11 614 required. A different approach to obtaining high
12
13 615 resolution STED images without this power
14
15 616 dependence is gSTED (gated-STED) [132]. gSTED
16
17 617 uses a continuous wave (CW) laser for the depletion
18
19 618 beam rather than a pulsed laser. When a CW
20
21 619 depletion beam is combined with a pulsed excitation
22
23 620 beam, spatial information about the underlying
24
25 621 fluorophore distribution becomes encoded in the
26
27 622 temporal information of emission on a nanosecond
28
29 623 timescale. By using time-gated detectors, photons
30
31 624 detected immediately after excitation can be
32
33 625 excluded from the final image, which improves
34
35 626 image resolution. By tuning the size of the time-gate,
36
37 627 gSTED can thus increase STED resolution
38
39 628 independent of increasing light dose to the sample
40
41 629 [133].
42
43 630 SIM is generally considered the least phototoxic
44
45 631 SRM technique [134]. However, it still requires the
46
47 632 acquisition of several frames (often ≥ 9) at high SNR
48
49 633 in order to generate the final reconstructed image.
50
51 634 Several approaches have been developed to reduce
52
53 635 the number of frames required for a SIM
54
55 636 reconstruction, including pixel reassignment and
56
57 637 image scanning microscopy (ISM) methods. One
58
59 638 example is multifocal structured illumination
60
639 microscopy (MSIM, [135]), which combines
640 principles from SIM and confocal microscopy to
641 scan an array of spots across the sample for fast
642 live-cell imaging with resolution doubling (**Fig. 5b**,
643 'Multi-focal illumination'). Another method, rapid

644 non-linear ISM [136], combines ISM with two-photon
645 excitation and second-harmonic generation for low
646 phototoxicity imaging. A wide range of such SIM-
647 based techniques exist, and have been rigorously
648 compared elsewhere [134], [137]. It has been
649 demonstrated recently that using sub-millisecond
650 pulses as excitation in SIM (when combined with
651 novel analytics as described below) reduced
652 photobleaching and enables long-term live-cell
653 imaging [138].
654 Techniques that restrict illumination to only the focal
655 plane of the sample are also preferable to those
656 which illuminate along the whole beam path. One
657 such example of this is TIRF (total internal reflection
658 fluorescence) microscopy, where only fluorophores
659 within a few hundred nanometers of the coverslip
660 are illuminated. While TIRF has been combined with
661 super-resolution modalities, such as SIM, and is
662 effective in reducing photodamage by axially
663 confining excitation [134], it is restrictive in that only
664 biological structures adjacent to the cell membrane
665 can be studied.
666 Light-sheet microscopy approaches similarly
667 confine illumination to a narrow band, but their
668 imaging geometries allow for investigation of
669 structures throughout the whole sample and not just
670 regions close to the coverslip. The majority of them
671 involve illuminating the sample with a thin sheet of
672 light and then detecting the fluorescence
673 perpendicular to the direction of sheet propagation
674 (**Fig. 5c**, 'Gaussian light sheet') [139], [140]. This
675 confers low phototoxicity as only the part of the
676 sample being imaged is illuminated without the need
677 for non-linear optical processes (which is the case in

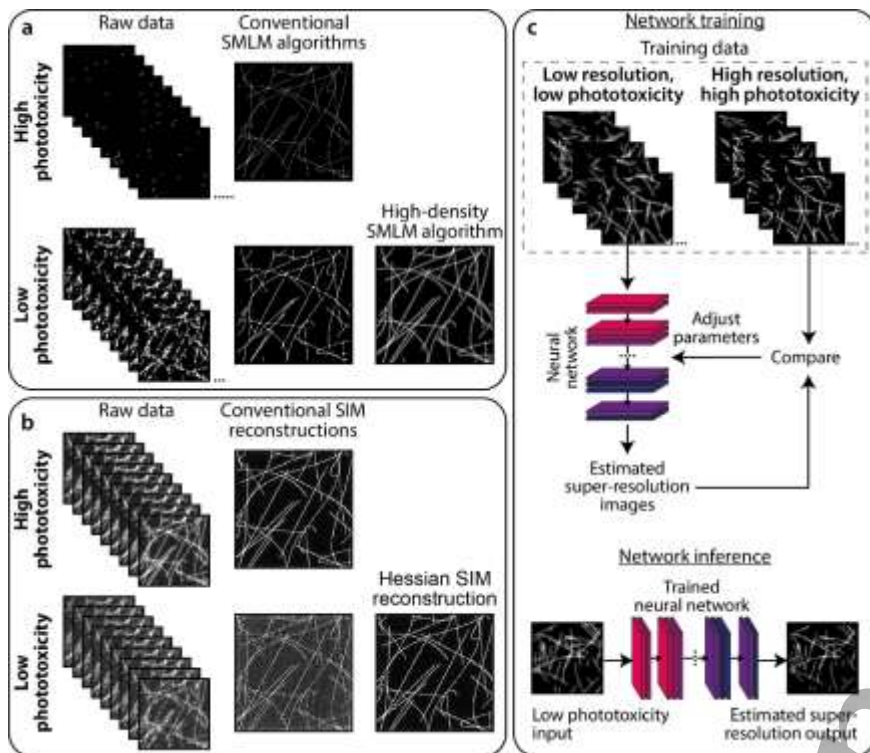


Fig. 6 Analytics to complement low-phototoxicity imaging regimes. **a** Top: typical SMLM images are successfully reconstructed from sparse blinking raw data acquired under high phototoxic illumination. Bottom: reducing phototoxic illumination leads to more emitting fluorophores per raw data frame. When reconstructed using conventional SMLM algorithms, these produce low-quality images containing artefacts. High density SMLM algorithms can produce better quality images from such datasets. **b** Top: typical SIM imaging involves acquiring 9-25 raw images (depending on the number of grating rotations and phases) at high SNR, which can be successfully reconstructed using conventional SIM algorithms. Bottom: decreasing the illumination intensity, and thus SNR of the raw images, leads to artefacts in images reconstructed using conventional methods. The Hessian SIM deconvolution algorithm can bypass this limitation [138]. **c** Deep neural networks can be trained to infer super-resolution information from e.g. low-resolution diffraction-limited or low-quality super-resolution images. In this example, a neural network can be trained on pairs of low resolution/super-resolution images of the trained structure ('Network training'). The trained network can then be applied to unseen low resolution images to infer the super-resolution equivalents ('Network inference').

678 two-photon microscopy). Indeed, light-sheet
 679 microscopy was named the Nature Methods
 680 technique of the year in 2014, in part due to its low
 681 phototoxicity [141]. There are several ways in which
 682 light-sheet microscopy schemes can yield super-
 683 resolution with reduced phototoxicity. Super-
 684 resolution in live samples has been demonstrated
 685 using light-sheet microscopy by simply combining
 686 this illumination geometry with SRM techniques
 687 such as SMLM [142]–[144] and RESOLFT [145].
 688 However, the employed SRM methods still require
 689 high-intensity illumination, and thus such composite
 690 techniques do not exploit the inherent low
 691 phototoxicity of light-sheet imaging. Therefore, a
 692 more elegant approach involves illuminating the
 693 sample with a light-sheet regime followed by the
 694 application of SMLM analytics designed for ultra-
 695 high-density datasets, which allows for reduction of
 696 the illumination power ([146] and **Analytics** section,
 697 see below). The more widely-explored method for

698 combining SRM and light-sheet microscopy has
 699 been the use of novel methods for generating and
 700 shaping the light-sheet. Bessel beams have been
 701 used to generate thinner light-sheets [147], and
 702 these beams have also been extended to
 703 incorporate SIM [148]. The latter strategy has also
 704 been demonstrated on a system with two
 705 counterpropagating light-sheets formed using
 706 standard Gaussian beams [149]. The most radical
 707 and live-imaging-friendly light-sheet SRM technique
 708 developed to date is lattice light-sheet microscopy
 709 [150] (**Fig. 5c**, 'Lattice light sheet'). This has
 710 demonstrated 3D time-lapse super-resolution
 711 imaging in both cultured cells and intact model
 712 organisms with minimal phototoxicity.
 713 An interesting approach to reducing the illumination
 714 dose in SRM is using spatially varying illumination
 715 depending on the structural content of the imaging
 716 region (**Fig. 5b**, 'Spatially adaptive illumination').
 717 This approach was originally demonstrated for

1
2
3 718 confocal imaging [48] and has since been extended
4
5 719 to SIM [151], RESOLFT [152] and indeed light-sheet
6
7 720 microscopy [141]. There is also a range of adaptive
8
9 721 illumination STED techniques that have been
10
11 722 developed [153]–[155], and while these
12
13 723 predominantly focus on reducing light dose in the
14
15 724 context of photobleaching, this will concomitantly
16
17 725 also impact the live-cell compatibility of these
18
19 726 techniques.

727 **Analytical approaches to live-cell Super-** 728 **Resolution Microscopy**

729 Analytics can be used to extract super-resolution
730 information from images acquired at low
731 illumination, and thus low phototoxicity (**Fig. 6**). Such
732 techniques are generally based on SMLM principles
733 but improve its live-cell compatibility (**Fig. 6a**). In
734 SMLM, when high intensity illumination is used,
735 fluorophore blinking is sparse and thus the well-
736 separated single molecules are straightforward to
737 detect and localise with high accuracy and precision
738 [156], [157]. However, as intensity is decreased
739 towards a lower phototoxicity regime, blinking
740 becomes more dense and molecules become
741 increasingly overlapped. Such datasets require
742 specialised algorithms to extract molecule locations.
743 The first example of such an algorithm was Super-
744 Resolution Optical Fluctuation imaging (SOFI),
745 where the temporal statistics of fluorophore intensity
746 oscillations are used to generate images with sub-
747 diffraction resolution [158]. Indeed, SOFI has been
748 used to image live cells [159] although only for short
749 periods of time due to the requirement for UV
750 illumination to induce photoswitching. Another

751 algorithm developed for analysing datasets with
752 dense blinking is 3B [160], where super-resolution
753 images can be obtained from datasets imaged with
754 a xenon arc lamp rather than lasers. However, both
755 SOFI and 3B techniques still rely on
756 photoswitchable fluorophores, which have
757 drawbacks discussed above. The Super-Resolution
758 Radial Fluctuations (SRRF) algorithm allows for the
759 reconstruction of super-resolution images from
760 datasets containing non-photoswitchable
761 fluorophores such as GFP [161], [162]. SRRF has
762 been shown to work on datasets obtained with
763 confocal and LED-illuminated microscopes, with the
764 latter enabling continuous live-cell imaging for >30
765 minutes [163]. However, SRRF cannot retrieve
766 resolutions in these regimes as high as those
767 achievable with photoswitchable fluorophores. A
768 promising new development for analysing high-
769 density datasets is Haar wavelet kernel (HAWK)
770 [164]. HAWK is a pre-processing algorithm that
771 separates fluorophores in time; this creates an
772 artificial lower-density dataset, which can then be
773 analysed using any SMLM algorithm.
774 While most analytical developments for live-cell
775 SRM centre on SMLM-based techniques, there are
776 also analytics for enabling lower phototoxicity
777 imaging in SIM and STED. Hessian-SIM is a
778 deconvolution algorithm that can obtain high-quality
779 SIM images from raw data acquired at low signal-to-
780 noise ratio (**Fig. 6b**) [138]. This overcomes a
781 substantial barrier in SIM, in that conventional SIM
782 reconstruction algorithms perform poorly on low-
783 illumination datasets, leading to artefacts within the
784 resulting images. Approaches have also been

785 proposed for low-power STED microscopy based on
786 reconstructing images with knowledge of
787 fluorescence lifetime changes induced by the STED
788 beam [75], [165].

789 A rapidly evolving field in microscopy image analysis
790 is the use of machine learning (ML)-based
791 techniques [166], [167]. Such techniques are used
792 for diverse applications including object
793 segmentation, denoising, and structure prediction,
794 and these can also be extended to SRM (**Fig. 6c**).

795 One example is Content Aware Image Restoration
796 (CARE), where a neural network is trained on high
797 illumination intensity datasets (i.e. high
798 phototoxicity) and used to denoise corresponding
799 datasets acquired at much lower illumination
800 intensities [168]. CARE was demonstrated to
801 enhance resolution of GFP-tagged microtubules to
802 a similar extent to SRRF analysis of the same data,
803 but with higher quality and higher temporal
804 resolution. There are also specialised ML algorithms
805 for super-resolution applications. ANNA-PALM is a
806 method that, after training a neural network with
807 sparse SMLM data, can reconstruct super-
808 resolution images from dense data and a
809 correspondingly lower number of frames [169].

810 While not demonstrated in live-cell data, this
811 technique could in theory alleviate phototoxicity with
812 minimal sacrifice to spatial resolution by imaging
813 photoswitchable FPs with lower illumination
814 intensity. Other ML-based techniques have also
815 allowed for prediction of enhanced resolution
816 images from low illumination diffraction-limited
817 images (**Fig. 6c**), for example: converting confocal

818 to Airyscan-type or STED-type images [75], [170]; or
819 widefield to SIM-type images [75].

820 **Discussion and outlook**

821 High quality live-cell fluorescence microscopy
822 involves compromising between four key properties:
823 SNR, imaging speed, spatial resolution, and sample
824 health [12]. We present an overview of the
825 challenges faced on how to balance the latter two
826 properties in live-cell SRM, highlighting potential
827 strategies to maximise resolution while minimising
828 phototoxicity.

829 As commercial super-resolution systems become
830 commonplace in biological labs and open-source
831 microscope hardware becomes more widespread,
832 there is a growing desire to translate cell biology
833 experiments from conventional diffraction-limited
834 microscopes to higher resolution alternatives.
835 However, the cost of this increased resolution is
836 often the sample health. Users must be aware of
837 what phototoxicity is, how to detect it, and methods
838 that can be used to ameliorate it. Unfortunately,
839 there are very few dedicated studies discussing
840 phototoxicity specifically in SRM [10], [29].

841 It is clear that there are several frontiers for
842 optimising SRM protocols for minimising
843 phototoxicity, and a much-needed development in
844 the field is a non-perturbing robust indicator of
845 sample health during imaging. Caution must be
846 taken when reporting and evaluating phototoxicity
847 as it would also require using uniform metrics for
848 data quality. There is already software available for
849 assessing the quality and resolution of SRM images
850 [171], [172] Comparative analytics for phototoxicity

1
2
3 851 would thus provide a complete numerical framework
4
5 852 for experiment optimisation.

6 853 As super-resolution microscopes become
7
8 854 increasingly standard equipment in biological
9
10 855 research, users must be aware of their limitations in
11
12 856 live-cell imaging. Many of the suggestions offered in
13
14 857 this review for reducing phototoxicity remain under
15
16 858 active development, and it is imperative for users to
17
18 859 follow progress in hardware, analytics and
19
20 860 fluorophores to ensure that they are minimising
21
22 861 photodamage to samples.

22 862 **Acknowledgements**

23
24 863 This work was funded by grants from the UK
25 864 Biotechnology and Biological Sciences Research
26 865 Council (BB/R000697/1; BB/R021805/1;
27 866 BB/S507532/1) (R.H.), the UK Medical Research
28 867 Council (MR/K015826/1) (R.H.), the Wellcome Trust

868 (203276/Z/16/Z) (S.C., R.H). K.L.T. supported by a
869 4-year MRC Research Studentship and Y.Y. by a 4-
870 year BBSRC Research Studentship. We would like
871 to thank Dr. David Albrecht (Max Planck Institute for
872 the Science of Light, Erlangen, Germany), Dr.
873 Francesca Bottanelli (Freie Universität Berlin, Berlin,
874 Germany), Dr. Agathe Chaigne (UCL, London, UK),
875 Dr. Gautam Dey (UCL, London, UK), Dr. Caron
876 Jacobs (University of Cape Town, Cape Town,
877 South Africa), Ms. Megan Jones (UCL, London, UK),
878 Dr. Christophe Leterrier (Aix Marseille Université,
879 Marseille, France), Dr. Apostolos Papandreou (UCL,
880 London, UK) and Dr. Uwe Schmidt (Max Planck
881 Institute of Molecular Cell Biology and Genetics,
882 Dresden, Germany) for valuable advice and
883 feedback.

884 885 **ORCID IDs**

886 Kalina L. Tosheva:
887 <https://orcid.org/0000-0003-0999-5182>
888 Yue Yuan:
889 <https://orcid.org/0000-0002-6698-3009>
890 Pedro Matos Pereira:
891 <https://orcid.org/0000-0002-1426-9540>
892 Siân Culley:
893 <https://orcid.org/0000-0003-2112-0143>
894 Ricardo Henriques:
895 <https://orcid.org/0000-0002-2043-5234>

896 **Bibliography**

- 897 [1] L. Schermelleh *et al.*, "Super-resolution microscopy demystified," *Nat. Cell Biol.*, vol. 21, no. 1, pp. 72–84,
898 2019.
- 899 [2] E. Betzig *et al.*, "Imaging Intracellular Fluorescent Proteins at Nanometer Resolution," *Science (80-.)*,
900 vol. 313, no. 5793, pp. 1642–1645, 2006.
- 901 [3] M. J. Rust, M. Bates, and X. Zhuang, "Sub-diffraction-limit imaging by stochastic optical reconstruction
902 microscopy (STORM)," *Nat. Methods*, vol. 3, no. 10, pp. 793–796, 2006.
- 903 [4] M. G. L. Gustafsson, "Surpassing the lateral resolution limit by a factor of two using structured
904 illumination microscopy," *J. Microsc.*, vol. 198, no. 2, pp. 82–87, May 2000.
- 905 [5] S. W. Hell and J. Wichmann, "Breaking the diffraction resolution limit by stimulated emission: stimulated-
906 emission-depletion fluorescence microscopy," *Opt. Lett.*, vol. 19, no. 11, pp. 780–782, Jun. 1994.
- 907 [6] K. Xu, G. Zhong, and X. Zhuang, "Actin, Spectrin, and Associated Proteins Form a Periodic Cytoskeletal
908 Structure in Axons," *Science (80-.)*, vol. 339, no. 6118, pp. 452 LP – 456, Jan. 2013.
- 909 [7] J. Nixon-Abell *et al.*, "Increased spatiotemporal resolution reveals highly dynamic dense tubular matrices
910 in the peripheral ER," *Science (80-.)*, vol. 354, no. 6311, p. aaf3928, Oct. 2016.
- 911 [8] J. Chojnacki *et al.*, "Envelope glycoprotein mobility on HIV-1 particles depends on the virus maturation
912 state," *Nat. Commun.*, vol. 8, no. 1, p. 545, 2017.
- 913 [9] T. Nerreter *et al.*, "Super-resolution microscopy reveals ultra-low CD19 expression on myeloma cells that
914 triggers elimination by CD19 CAR-T," *Nat. Commun.*, vol. 10, no. 1, p. 3137, 2019.
- 915 [10] S. Wäldchen, J. Lehmann, T. Klein, S. van de Linde, and M. Sauer, "Light-induced cell damage in live-
916 cell super-resolution microscopy," *Sci. Rep.*, vol. 5, p. 15348, Oct. 2015.
- 917 [11] R. Henriques, C. Griffiths, E. Hesper Rego, and M. M. Mhlanga, "PALM and STORM: Unlocking live-cell
918 super-resolution," *Biopolymers*, vol. 95, no. 5, pp. 322–331, May 2011.
- 919 [12] P. P. Laissue, R. A. Alghamdi, P. Tomancak, E. G. Reynaud, and H. Shroff, "Assessing phototoxicity in
920 live fluorescence imaging," *Nat. Methods*, vol. 14, p. 657, Jun. 2017.
- 921 [13] J. Icha, M. Weber, J. C. Waters, and C. Norden, "Phototoxicity in live fluorescence microscopy, and how
922 to avoid it," *BioEssays*, vol. 39, no. 8, p. 1700003, Aug. 2017.
- 923 [14] V. Magidson and A. Khodjakov, *Circumventing photodamage in live-cell microscopy*, 4th ed., vol. 114.
924 Elsevier Inc., 2013.
- 925 [15] R. Dixit and R. Cyr, "Cell damage and reactive oxygen species production induced by fluorescence
926 microscopy: effect on mitosis and guidelines for non-invasive fluorescence microscopy," *Plant J.*, vol. 36,
927 no. 2, pp. 280–290, 2003.
- 928 [16] K. Logg, K. Bodvard, A. Blomberg, and M. Käll, "Investigations on light-induced stress in fluorescence
929 microscopy using nuclear localization of the transcription factor Msn2p as a reporter," *FEMS Yeast Res.*,

- 1
2
3 930 vol. 9, no. 6, pp. 875–884, 2009.
- 4
5 931 [17] Y. Devary, C. Rosette, J. A. DiDonato, and M. Karin, “NF-kappa B activation by ultraviolet light not
6 932 dependent on a nuclear signal,” *Science* (80-), vol. 261, no. 5127, pp. 1442–1445, 1993.
- 7
8 933 [18] A. Rehemtulla, C. A. Hamilton, A. M. Chinnaiyan, and V. M. Dixit, “Ultraviolet Radiation-induced
9 934 Apoptosis Is Mediated by Activation of CD-95 (Fas/APO-1),” *J. Biol. Chem.* , vol. 272, no. 41, pp. 25783–
10 935 25786, Oct. 1997.
- 11
12
13 936 [19] M. J. Peak, J. G. Peak, and B. A. Carnes, “Induction of Direct and Indirect Single-Strand Breaks in
14 937 Human Cell Dna By Far- and Near-Ultraviolet Radiations: Action Spectrum and Mechanisms,”
15 938 *Photochem. Photobiol.*, vol. 45, no. 3, pp. 381–387, 1987.
- 16
17
18 939 [20] M. J. Peak and J. G. Peak, “SINGLE-STRAND BREAKS INDUCED IN BACILLUS SUBTILIS DNA BY
19 940 ULTRAVIOLET LIGHT: ACTION SPECTRUM and PROPERTIES,” *Photochem. Photobiol.*, vol. 35, no. 5,
20 941 pp. 675–680, May 1982.
- 21
22
23 942 [21] B. Durbeej and L. A. Eriksson, “Reaction mechanism of thymine dimer formation in DNA induced by UV
24 943 light,” *J. Photochem. Photobiol. A Chem.*, vol. 152, no. 1, pp. 95–101, 2002.
- 25
26
27 944 [22] D. E. Brash *et al.*, “A role for sunlight in skin cancer: UV-induced p53 mutations in squamous cell
28 945 carcinoma,” *Proc. Natl. Acad. Sci.*, vol. 88, no. 22, pp. 10124–10128, 1991.
- 29
30
31 946 [23] H. Vrieling *et al.*, “DNA strand specificity for UV-induced mutations in mammalian cells.,” *Mol. Cell. Biol.*,
32 947 vol. 9, no. 3, pp. 1277–1283, 1989.
- 33
34 948 [24] M. L. Cunningham, J. S. Johnson, S. M. Giovanazzi, and M. J. Peak, “Photosensitized Production of
35 949 Superoxide Anion by Monochromatic (290–405 nm) Ultraviolet Irradiation of NADH and NADPH
36 950 Coenzymes,” *Photochem. Photobiol.*, vol. 42, no. 2, pp. 125–128, 1985.
- 37
38
39 951 [25] M. Eichler, R. Lavi, A. Shainberg, and R. Lubart, “Flavins are source of visible-light-induced free radical
40 952 formation in cells,” *Lasers Surg. Med.*, vol. 37, no. 4, pp. 314–319, Oct. 2005.
- 41
42
43 953 [26] P. E. Hockberger *et al.*, “Activation of flavin-containing oxidases underlies light-induced production of
44 954 H₂O₂ in mammalian cells,” *Proc. Natl. Acad. Sci.*, vol. 96, no. 11, pp. 6255–6260, 1999.
- 45
46 955 [27] G. Y. Fraikin, M. G. Strakhovskaya, and A. B. Rubin, “The role of membrane-bound porphyrin-type
47 956 compound as endogenous sensitizer in photodynamic damage to yeast plasma membranes,” *J.*
48 957 *Photochem. Photobiol. B Biol.*, vol. 34, no. 2–3, pp. 129–135, 1996.
- 49
50
51 958 [28] F. Ricchelli, “Photophysical properties of porphyrins in biological membranes,” *J. Photochem. Photobiol.*
52 959 *B Biol.*, vol. 29, no. 2, pp. 109–118, 1995.
- 53
54
55 960 [29] N. Kilian *et al.*, “Assessing photodamage in live-cell STED microscopy,” *Nat. Methods*, vol. 15, no. 10, pp.
56 961 755–756, 2018.
- 57
58 962 [30] C. S. Foote, “DEFINITION OF TYPE I and TYPE II PHOTSENSITIZED OXIDATION,” *Photochem.*
59 963 *Photobiol.*, vol. 54, no. 5, p. 659, Nov. 1991.

- 1
2
3 964 [31] W. C. Burhans and N. H. Heintz, "The cell cycle is a redox cycle: Linking phase-specific targets to cell
4 fate," *Free Radic. Biol. Med.*, vol. 47, no. 9, pp. 1282–1293, 2009.
5 965
6 966 [32] Z. Schilling *et al.*, "Predictive-focus illumination for reducing photodamage in live-cell microscopy," *J.*
7 *Microsc.*, vol. 246, no. 2, pp. 160–167, May 2012.
8 967
9 968 [33] S. Douthwright and G. Sluder, "Live Cell Imaging: Assessing the Phototoxicity of 488 and 546 nm Light
10 and Methods to Alleviate it," *J. Cell. Physiol.*, vol. 232, no. 9, pp. 2461–2468, 2017.
11 969
12 970 [34] J.-Y. Tinevez *et al.*, "Chapter fifteen - A Quantitative Method for Measuring Phototoxicity of a Live Cell
13 Imaging Microscope," in *Imaging and Spectroscopic Analysis of Living Cells*, vol. 506, P. M. B. T.-M. in E.
14 Conn, Ed. Academic Press, 2012, pp. 291–309.
15 971
16 972 [35] P. M. Carlton *et al.*, "Fast live simultaneous multiwavelength four-dimensional optical microscopy," *Proc.*
17 *Natl. Acad. Sci.*, vol. 107, no. 37, pp. 16016–16022, 2010.
18 973
19 974 [36] M. M. Knight, S. R. Roberts, D. A. Lee, and D. L. Bader, "Live cell imaging using confocal microscopy
20 induces intracellular calcium transients and cell death," *Am. J. Physiol. Physiol.*, vol. 284, no. 4, pp.
21 C1083–C1089, Apr. 2003.
22 975
23 976 [37] Y. Wu *et al.*, "Inverted selective plane illumination microscopy (iSPIM) enables coupled cell identity
24 lineaging and neurodevelopmental imaging in *Caenorhabditis elegans*," *Proc. Natl. Acad. Sci.*, vol. 108,
25 no. 43, pp. 17708–17713, 2011.
26 977
27 978 [38] H. Schneckenburger *et al.*, "Light exposure and cell viability in fluorescence microscopy," *J. Microsc.*, vol. 108,
28 no. 43, pp. 17708–17713, 2011.
29 979
30 980 [39] R. Cole, "Live-cell imaging," *Cell Adh. Migr.*, vol. 8, no. 5, pp. 452–459, Sep. 2014.
31 981
32 982 [40] F. Mubaid and C. M. Brown, "Less is More: Longer Exposure Times with Low Light Intensity is Less
33 Photo-Toxic," *Micros. Today*, vol. 25, no. 6, pp. 26–35, 2017.
34 983
35 984 [41] C. Boudreau, T. L. Wee, Y. R. Duh, M. P. Couto, K. H. Ardakani, and C. M. Brown, "Excitation light dose
36 engineering to reduce photo-bleaching and photo-toxicity," *Sci. Rep.*, vol. 6, pp. 1–12, 2016.
37 985
38 986 [42] Y. Wu, X. Wu, R. Lu, J. Zhang, L. Toro, and E. Stefani, "Resonant Scanning with Large Field of View
39 Reduces Photobleaching and Enhances Fluorescence Yield in STED Microscopy," *Sci. Rep.*, vol. 5, p.
40 14766, Oct. 2015.
41 987
42 988 [43] E. A. Halabi, D. Pinotsi, and P. Rivera-Fuentes, "Photoregulated fluxional fluorophores for live-cell super-
43 resolution microscopy with no apparent photobleaching," *Nat. Commun.*, vol. 10, no. 1, p. 1232, 2019.
44 989
45 990 [44] K. Jacobson, Z. Rajfur, E. Vitriol, and K. Hahn, "Chromophore-assisted laser inactivation in cell biology,"
46 *Trends Cell Biol.*, vol. 18, no. 9, pp. 443–450, 2008.
47 991
48 992 [45] J. H. Stockley *et al.*, "Surpassing light-induced cell damage in vitro with novel cell culture media," *Sci.*
49 *Rep.*, vol. 7, no. 1, p. 849, 2017.
50 993
51 994 [46] J. W. Dobrucki, D. Feret, and A. Noatynska, "Scattering of exciting light by live cells in fluorescence
52
53
54
55
56
57
58
59
60

- 1
2
3 998 confocal imaging: Phototoxic effects and relevance for FRAP studies," *Biophys. J.*, vol. 93, no. 5, pp.
4 999 1778–1786, 2007.
- 6 1000 [47] C. Roehlecke, A. Schaller, L. Knels, and R. H. W. Funk, "The Influence of Sublethal Blue Light Exposure
7 1001 on Human {{RPE}} Cells," *Mol. Vis.*, vol. 15, pp. 1929–1938, 2009.
- 10 1002 [48] R. A. Hoebe, C. H. Van Oven, T. W. J. Gadella, P. B. Dhonukshe, C. J. F. Van Noorden, and E. M. M.
11 1003 Manders, "Controlled light-exposure microscopy reduces photobleaching and phototoxicity in
12 1004 fluorescence live-cell imaging," *Nat. Biotechnol.*, vol. 25, no. 2, pp. 249–253, 2007.
- 15 1005 [49] J. Ge *et al.*, "Standard fluorescent imaging of live cells is highly genotoxic," *Cytom. Part A*, vol. 83A, no.
16 1006 6, pp. 552–560, Jun. 2013.
- 18 1007 [50] D. H. Hawkins and H. Abrahamse, "The role of laser fluence in cell viability, proliferation, and membrane
19 1008 integrity of wounded human skin fibroblasts following helium-neon laser irradiation," *Lasers Surg. Med.*,
20 1009 vol. 38, no. 1, pp. 74–83, Jan. 2006.
- 23 1010 [51] Y. Kuse, K. Ogawa, K. Tsuruma, M. Shimazawa, and H. Hara, "Damage of photoreceptor-derived cells in
24 1011 culture induced by light emitting diode-derived blue light," *Sci. Rep.*, vol. 4, pp. 1–12, 2014.
- 27 1012 [52] A. McDonald, J. Harris, D. MacMillan, J. Dempster, and G. McConnell, "Light-induced Ca²⁺ transients
28 1013 observed in widefield epi-fluorescence microscopy of excitable cells," *Biomed. Opt. Express*, vol. 3, no. 6,
29 1014 p. 1266, 2012.
- 32 1015 [53] H. J. Koester, D. Baur, R. Uhl, and S. W. Hell, "Ca²⁺ fluorescence imaging with pico- and femtosecond
33 1016 two-photon excitation: Signal and photodamage," *Biophys. J.*, vol. 77, no. 4, pp. 2226–2236, 1999.
- 36 1017 [54] A. Hopt and E. Neher, "Highly Nonlinear Photodamage in Two-Photon Fluorescence Microscopy,"
37 1018 *Biophys. J.*, vol. 80, no. 4, pp. 2029–2036, 2001.
- 39 1019 [55] C.-H. Chuang, A. E. Carpenter, B. Fuchsova, T. Johnson, P. de Lanerolle, and A. S. Belmont, "Long-
40 1020 Range Directional Movement of an Interphase Chromosome Site," *Curr. Biol.*, vol. 16, no. 8, pp. 825–
41 1021 831, 2006.
- 44 1022 [56] T. Minamikawa, D. A. Williams, D. N. Bowser, and P. Nagley, "Mitochondrial Permeability Transition and
45 1023 Swelling Can Occur Reversibly without Inducing Cell Death in Intact Human Cells," *Exp. Cell Res.*, vol.
46 1024 246, no. 1, pp. 26–37, 1999.
- 49 1025 [57] R. A. Hoebe, H. T. M. van der Voort, J. Stap, C. J. F. van Noorden, and E. M. M. Manders, "Quantitative
50 1026 determination of the reduction of phototoxicity and photobleaching by controlled light exposure
51 1027 microscopy," *J. Microsc.*, vol. 231, no. 1, pp. 9–20, Jul. 2008.
- 54 1028 [58] D. Richmond, A. P.-T. Jost, T. Lambert, J. Waters, and H. Elliott, "DeadNet: Identifying Phototoxicity from
55 1029 Label-free Microscopy Images of Cells using Deep ConvNets," *CoRR*, vol. abs/1701.0, 2017.
- 58 1030 [59] G. Vicidomini, P. Bianchini, and A. Diaspro, "STED super-resolved microscopy," *Nat. Methods*, vol. 15,
59 1031 no. 3, pp. 173–182, 2018.

- 1
2
3 1032 [60] R. Henriques and M. M. Mhlanga, "PALM and STORM: What hides beyond the Rayleigh limit?,"
4
5 1033 *Biotechnol. J.*, vol. 4, no. 6, pp. 846–857, Jun. 2009.
- 6 1034 [61] J. C. Chozinski, Tyler J., Gagnon, Lauren A., Vaughan, "Twinkle, twinkle little star: photoswitchable
7
8 1035 fluorophores for super-resolution imaging," *FEBS Lett.*, vol. 588, p. 3603, 2014.
- 9
10 1036 [62] G. T. Dempsey, J. C. Vaughan, K. H. Chen, M. Bates, and X. Zhuang, "Evaluation of fluorophores for
11
12 1037 optimal performance in localization-based super-resolution imaging," *Nat. Methods*, vol. 8, no. 12, pp.
13
14 1038 1027–1040, 2011.
- 15 1039 [63] J. V. Thevathasan *et al.*, "Nuclear pores as versatile reference standards for quantitative superresolution
16
17 1040 microscopy," *bioRxiv*, 2019.
- 18 1041 [64] S. van de Linde, I. Krstić, T. Prisner, S. Doose, M. Heilemann, and M. Sauer, "Photoinduced formation of
19
20 1042 reversible dye radicals and their impact on super-resolution imaging.," *Photochem. Photobiol. Sci.*, vol.
21
22 1043 10, no. 4, pp. 499–506, 2011.
- 23
24 1044 [65] N. C. Shaner *et al.*, "A bright monomeric green fluorescent protein derived from *Branchiostoma*
25
26 1045 *lanceolatum*," *Nat. Methods*, vol. 10, no. 5, pp. 407–409, 2013.
- 27 1046 [66] D. S. Bindels *et al.*, "mScarlet: a bright monomeric red fluorescent protein for cellular imaging," *Nat.*
28
29 1047 *Methods*, vol. 14, no. 1, pp. 53–56, 2017.
- 30 1048 [67] A. Hense, B. Prunsche, P. Gao, Y. Ishitsuka, K. Nienhaus, and G. U. Nienhaus, "Monomeric Garnet, a
31
32 1049 far-red fluorescent protein for live-cell STED imaging," *Sci. Rep.*, vol. 5, pp. 1–10, 2015.
- 33
34 1050 [68] M. Zhang *et al.*, "Rational design of true monomeric and bright photoactivatable fluorescent proteins,"
35
36 1051 *Nat. Methods*, vol. 9, no. 7, pp. 727–729, 2012.
- 37 1052 [69] A. B. Rosenbloom, S.-H. S.-H. Lee, M. To, A. Lee, J. Y. Shin, and C. Bustamante, "Optimized two-color
38
39 1053 super resolution imaging of Drp1 during mitochondrial fission with a slow-switching Dronpa variant," *Proc.*
40
41 1054 *Natl. Acad. Sci.*, vol. 111, no. 36, pp. 13093–13098, 2014.
- 42
43 1055 [70] Y. Arai *et al.*, "Spontaneously Blinking Fluorescent Protein for Simple Single Laser Super-Resolution Live
44
45 1056 Cell Imaging," *ACS Chem. Biol.*, p. acschembio.8b00200, 2018.
- 46 1057 [71] W. P. Dempsey *et al.*, "In vivo single-cell labeling by confined primed conversion," *Nat. Methods*, vol. 12,
47
48 1058 no. 7, pp. 645–648, 2015.
- 49 1059 [72] M. A. Mohr and P. Pantazis, "Primed Conversion: The New Kid on the Block for Photoconversion,"
50
51 1060 *Chem. – A Eur. J.*, vol. 24, no. 33, pp. 8268–8274, Jun. 2018.
- 52
53 1061 [73] B. Turkowyd *et al.*, "A General Mechanism of Photoconversion of Green-to-Red Fluorescent Proteins
54
55 1062 Based on Blue and Infrared Light Reduces Phototoxicity in Live-Cell Single-Molecule Imaging," *Angew.*
56
57 1063 *Chemie - Int. Ed.*, vol. 56, no. 38, pp. 11634–11639, 2017.
- 58 1064 [74] X. Zhang *et al.*, "Highly photostable, reversibly photoswitchable fluorescent protein with high contrast
59
60 1065 ratio for live-cell superresolution microscopy," *Proc. Natl. Acad. Sci.*, vol. 113, no. 37, pp. 10364–10369,

- 1
2
3 1066 2016.
4
5 1067 [75] S. Wang *et al.*, "GMars-T Enabling Multimodal Subdiffraction Structural and Functional Fluorescence
6 1068 Imaging in Live Cells," *Anal. Chem.*, vol. 90, pp. 6626–6634, 2018.
7
8 1069 [76] M. V Sednev, C. A. Wurm, V. N. Belov, and S. W. Hell, "Carborhodol: A New Hybrid Fluorophore
9 1070 Obtained by Combination of Fluorescein and Carbopyronine Dye Cores," *Bioconjug. Chem.*, vol. 24, no.
10 1071 4, pp. 690–700, Apr. 2013.
11
12 1072 [77] J. B. Grimm *et al.*, "A general method to fine-tune fluorophores for live-cell and in vivo imaging," *Nat.*
13 1073 *Methods*, vol. 14, p. 987, Sep. 2017.
14
15 1074 [78] P. Mateos-Gil, S. Letschert, S. Doose, and M. Sauer, "Super-Resolution Imaging of Plasma Membrane
16 1075 Proteins with Click Chemistry," *Front. Cell Dev. Biol.*, vol. 4, no. September, p. 98, 2016.
17
18 1076 [79] A. D. Thompson *et al.*, "Long-Term Live-Cell STED Nanoscopy of Primary and Cultured Cells with the
19 1077 Plasma Membrane HIDE Probe Dil-SiR.," *Angew. Chem. Int. Ed. Engl.*, vol. 56, no. 35, pp. 10408–
20 1078 10412, Aug. 2017.
21
22 1079 [80] G. Lukinavičius *et al.*, "Fluorogenic probes for live-cell imaging of the cytoskeleton," *Nat. Methods*, vol.
23 1080 11, no. 7, pp. 731–733, 2014.
24
25 1081 [81] E. Kozma and P. Kele, "Fluorogenic probes for super-resolution microscopy," *Org. Biomol. Chem.*, vol.
26 1082 17, no. 2, pp. 215–233, 2019.
27
28 1083 [82] S.-H. Shim *et al.*, "Super-resolution fluorescence imaging of organelles in live cells with photoswitchable
29 1084 membrane probes," *Proc. Natl. Acad. Sci.*, vol. 109, no. 35, pp. 13978–13983, 2012.
30
31 1085 [83] M. Collot *et al.*, "MemBright: A Family of Fluorescent Membrane Probes for Advanced Cellular Imaging
32 1086 and Neuroscience," *Cell Chem. Biol.*, vol. 26, no. 4, pp. 600-614.e7, 2019.
33
34 1087 [84] L. Wang, M. S. Frei, A. Salim, and K. Johnsson, "Small-Molecule Fluorescent Probes for Live-Cell Super-
35 1088 Resolution Microscopy," *J. Am. Chem. Soc.*, vol. 141, no. 7, pp. 2770–2781, Feb. 2019.
36
37 1089 [85] L. D. Lavis, "Teaching Old Dyes New Tricks: Biological Probes Built from Fluoresceins and Rhodamines,"
38 1090 *Annu. Rev. Biochem.*, vol. 86, no. 1, pp. 825–843, 2017.
39
40 1091 [86] A. Gautier *et al.*, "An Engineered Protein Tag for Multiprotein Labeling in Living Cells," *Chem. Biol.*, vol.
41 1092 15, no. 2, pp. 128–136, Feb. 2008.
42
43 1093 [87] G. V Los *et al.*, "HaloTag: a novel protein labeling technology for cell imaging and protein analysis.," *ACS*
44 1094 *Chem. Biol.*, vol. 3, no. 6, pp. 373–82, Jun. 2008.
45
46 1095 [88] B. A. Griffin, S. R. Adams, and R. Y. Tsien, "Specific covalent labeling of recombinant protein molecules
47 1096 inside live cells.," *Science (80-.)*, vol. 281, no. 5374, pp. 269–72, Jul. 1998.
48
49 1097 [89] M. Lelek *et al.*, "Superresolution imaging of HIV in infected cells with FIAsH-PALM.," *Proc. Natl. Acad.*
50 1098 *Sci. U. S. A.*, vol. 109, no. 22, pp. 8564–9, May 2012.
51
52 1099 [90] T. Stephan, A. Roesch, D. Riedel, and S. Jakobs, "Live-cell STED nanoscopy of mitochondrial cristae,"

- 1
2
3 1100 *Sci. Rep.*, vol. 9, no. 1, p. 12419, 2019.
- 4
5 1101 [91] S. N. Uno, D. K. Tiwari, M. Kamiya, Y. Arai, T. Nagai, and Y. Urano, "A guide to use photocontrollable
6 1102 fluorescent proteins and synthetic smart fluorophores for nanoscopy," *Microscopy*, vol. 64, no. 4, pp.
7 1103 263–277, 2015.
- 8
9
10 1104 [92] H. Takakura *et al.*, "Long time-lapse nanoscopy with spontaneously blinking membrane probes," *Nat.*
11 1105 *Biotechnol.*, vol. 35, no. 8, pp. 773–780, 2017.
- 12
13 1106 [93] C. Wang, M. Taki, Y. Sato, A. Fukazawa, T. Higashiyama, and S. Yamaguchi, "Super-Photostable
14 1107 Phosphole-Based Dye for Multiple-Acquisition Stimulated Emission Depletion Imaging," *J. Am. Chem.*
15 1108 *Soc.*, vol. 139, no. 30, pp. 10374–10381, 2017.
- 16
17
18 1109 [94] L. Chu *et al.*, "Two-color nanoscopy of organelles for extended times with HIDE probes," *bioRxiv*, 2019.
- 19
20 1110 [95] A. N. Butkevich *et al.*, "Hydroxylated Fluorescent Dyes for Live-Cell Labeling: Synthesis, Spectra and
21 1111 Super-Resolution STED.," *Chemistry (Easton)*, vol. 23, no. 50, pp. 12114–12119, Sep. 2017.
- 22
23 1112 [96] I. Nikić *et al.*, "Debugging Eukaryotic Genetic Code Expansion for Site-Specific Click-PAINT Super-
24 1113 Resolution Microscopy.," *Angew. Chem. Int. Ed. Engl.*, vol. 55, no. 52, pp. 16172–16176, Dec. 2016.
- 25
26
27 1114 [97] A. O. Khan, V. A. Simms, J. A. Pike, S. G. Thomas, and N. V Morgan, "CRISPR-Cas9 Mediated Labelling
28 1115 Allows for Single Molecule Imaging and Resolution.," *Sci. Rep.*, vol. 7, no. 1, p. 8450, Aug. 2017.
- 29
30 1116 [98] T. Schvartz *et al.*, "Direct fluorescent-dye labeling of α -tubulin in mammalian cells for live cell and
31 1117 superresolution imaging.," *Mol. Biol. Cell*, vol. 28, no. 21, pp. 2747–2756, Oct. 2017.
- 32
33
34 1118 [99] P. . B. T. . S. W. S. L. . W. R. . S. H. Wagner M.; Weber, "Light Dose is a Limiting Factor to Maintain Cell
35 1119 Viability in Fluorescence Microscopy and Single Molecule Detection," *Int. J. Mol. Sci.*, vol. 11, no. 3, pp.
36 1120 956–966, 2010.
- 37
38
39 1121 [100] M. E. Bulina, K. A. Lukyanov, O. V Britanova, D. Onichtchouk, S. Lukyanov, and D. M. Chudakov,
40 1122 "Chromophore-assisted light inactivation (CALI) using the phototoxic fluorescent protein KillerRed," *Nat.*
41 1123 *Protoc.*, vol. 1, no. 2, pp. 947–953, 2006.
- 42
43
44 1124 [101] M. M. Frigault, J. Lacoste, J. L. Swift, and C. M. Brown, "Live-cell microscopy - tips and tools," *J. Cell*
45 1125 *Sci.*, vol. 122, no. 6, pp. 753–767, 2009.
- 46
47
48 1126 [102] L. Song, E. J. Hennink, I. T. Young, and H. J. Tanke, "Photobleaching kinetics of fluorescein in
49 1127 quantitative fluorescence microscopy," *Biophys. J.*, vol. 68, no. 6, pp. 2588–2600, 1995.
- 50
51 1128 [103] J. W. Dobrucki, "Interaction of oxygen-sensitive luminescent probes Ru(phen)₃²⁺ and Ru(bipy)₃²⁺ with
52 1129 animal and plant cells in vitro: Mechanism of phototoxicity and conditions for non-invasive oxygen
53 1130 measurements," *J. Photochem. Photobiol. B Biol.*, vol. 65, no. 2, pp. 136–144, 2001.
- 54
55
56 1131 [104] J. A. Bloom and W. W. Webb, "Photodamage to intact erythrocyte membranes at high laser intensities:
57 1132 methods of assay and suppression.," *J. Histochem. Cytochem.*, vol. 32, no. 6, pp. 608–616, Jun. 1984.
- 58
59
60 1133 [105] C. M. Waterman-Storer, J. W. Sanger, and J. M. Sanger, "Dynamics of organelles in the mitotic spindles

- 1
2
3 1134 of living cells: Membrane and microtubule interactions," *Cell Motil.*, vol. 26, no. 1, pp. 19–39, Jan. 1993.
- 4
5 1135 [106] W. Xiang, M. J. Roberti, J.-K. Hériché, S. Huet, S. Alexander, and J. Ellenberg, "Correlative live and
6 1136 super-resolution imaging reveals the dynamic structure of replication domains," *J. Cell Biol.*, vol. 217, no.
7 1137 6, pp. 1973–1984, Jun. 2018.
- 8
9 1138 [107] R. Kohen and A. Nyska, "Invited Review: Oxidation of Biological Systems: Oxidative Stress Phenomena,
10 1139 Antioxidants, Redox Reactions, and Methods for Their Quantification," *Toxicol. Pathol.*, vol. 30, no. 6, pp.
11 1140 620–650, Oct. 2002.
- 12
13 1141 [108] T.-W. Wu *et al.*, "The cytoprotective effect of Trolox demonstrated with three types of human cells,"
14 1142 *Biochem. Cell Biol.*, vol. 68, no. 10, pp. 1189–1194, Oct. 1990.
- 15
16 1143 [109] I. Rasnik, S. A. McKinney, and T. Ha, "Nonblinking and long-lasting single-molecule fluorescence
17 1144 imaging," *Nat. Methods*, vol. 3, no. 11, pp. 891–893, 2006.
- 18
19 1145 [110] A. M. Bogdanov, E. I. Kudryavtseva, and K. A. Lukyanov, "Anti-Fading Media for Live Cell GFP Imaging,"
20 1146 *PLoS One*, vol. 7, no. 12, p. e53004, Dec. 2012.
- 21
22 1147 [111] P. Atkins and J. de Paula, *Physical Chemistry*, Eighth edit. New York, US: W.H. Freeman and Company,
23 1148 2006.
- 24
25 1149 [112] J. Widengren, A. Chmyrov, C. Eggeling, P.-Å. Löfdahl, and C. A. M. Seidel, "Strategies to Improve
26 1150 Photostabilities in Ultrasensitive Fluorescence Spectroscopy," *J. Phys. Chem. A*, vol. 111, no. 3, pp. 429–
27 1151 440, Jan. 2007.
- 28
29 1152 [113] H. Giloh and J. W. Sedat, "Fluorescence microscopy: reduced photobleaching of rhodamine and
30 1153 fluorescein protein conjugates by n-propyl gallate," *Science (80-.)*, vol. 217, no. 4566, pp. 1252–1255,
31 1154 Sep. 1982.
- 32
33 1155 [114] K. Valnes and P. Brandtzaeg, "Retardation of immunofluorescence fading during microscopy.," *J.*
34 1156 *Histochem. Cytochem.*, vol. 33, no. 8, pp. 755–761, Aug. 1985.
- 35
36 1157 [115] G. D. Johnson, R. S. Davidson, K. C. McNamee, G. Russell, D. Goodwin, and E. J. Holborow, "Fading of
37 1158 immunofluorescence during microscopy: a study of the phenomenon and its remedy," *J. Immunol.*
38 1159 *Methods*, vol. 55, no. 2, pp. 231–242, 1982.
- 39
40 1160 [116] A. Longin, C. Souchier, M. Ffrench, and P. A. Bryon, "Comparison of anti-fading agents used in
41 1161 fluorescence microscopy: image analysis and laser confocal microscopy study.," *J. Histochem.*
42 1162 *Cytochem.*, vol. 41, no. 12, pp. 1833–1840, Dec. 1993.
- 43
44 1163 [117] A. N. Fletcher and M. E. Pietrak, "Laser dye stability, part 10. Effects of DABCO on flashlamp pumping of
45 1164 coumarin dyes," *Appl. Phys. B*, vol. 37, no. 3, pp. 151–157, 1985.
- 46
47 1165 [118] M. Ono, T. Murakami, A. Kudo, M. Isshiki, H. Sawada, and A. Segawa, "Quantitative Comparison of Anti-
48 1166 Fading Mounting Media for Confocal Laser Scanning Microscopy," *J. Histochem. Cytochem.*, vol. 49, no.
49 1167 3, pp. 305–311, Mar. 2001.

- 1
2
3 1168 [119] A. M. Bogdanov, E. A. Bogdanova, D. M. Chudakov, T. V. Gorodnicheva, S. Lukyanov, and K. A.
4 Lukyanov, "Cell culture medium affects GFP photostability: a solution," *Nat. Methods*, vol. 6, no. 12, pp.
5 1169 859–860, 2009.
6 1170
7
8 1171 [120] A. M. Edwards, E. Silva, B. Jofré, M. I. Becker, and A. E. De Ioannes, "Visible light effects on tumoral
9 cells in a culture medium enriched with tryptophan and riboflavin," *J. Photochem. Photobiol. B Biol.*, vol.
10 1172 24, no. 3, pp. 179–186, 1994.
11 1173
12
13 1174 [121] A. Grzelak, B. Rychlik, and G. Bartosz, "Light-dependent generation of reactive oxygen species in cell
14 culture media," *Free Radic. Biol. Med.*, vol. 30, no. 12, pp. 1418–1425, 2001.
15 1175
16
17 1176 [122] G. T. Spierenburg, F. T. J. J. Oerlemans, J. P. R. M. Van Laarhoven, and C. H. M. M. De Bruyn,
18 "Phototoxicity of N-hydroxyethylpiperazine-N'-2-ethanesulfonic acid-buffered culture media for human
19 leukemic cell lines," *Cancer Res.*, vol. 44, pp. 2253–2254, 1984.
20 1178
21
22 1179 [123] J. S. Zigler, J. L. Lepe-Zuniga, B. Vistica, and I. Gery, "Analysis of the cytotoxic effects of light-exposed
23 hepes-containing culture medium," *Vitr. Cell. Dev. Biol.*, vol. 21, no. 5, pp. 282–287, 1985.
24 1180
25
26 1181 [124] P. Almada, S. Culley, and R. Henriques, "PALM and STORM: Into large fields and high-throughput
27 microscopy with sCMOS detectors," *Methods*, vol. 88, pp. 109–121, 2015.
28 1182
29 1183 [125] S. Herbert, H. Soares, C. Zimmer, and R. Henriques, "Single-Molecule Localization Super-Resolution
30 Microscopy: Deeper and Faster," *Microsc. Microanal.*, vol. 18, no. 6, pp. 1419–1429, 2012.
31 1184
32 1185 [126] P. Almada *et al.*, "Automating multimodal microscopy with NanoJ-Fluidics," *Nat. Commun.*, vol. 10, no. 1,
33 p. 1223, 2019.
34 1186
35
36 1187 [127] G. Donnert, C. Eggeling, and S. W. Hell, "Major signal increase in fluorescence microscopy through dark-
37 state relaxation," *Nat. Methods*, vol. 4, no. 1, pp. 81–86, 2007.
38 1188
39 1189 [128] K. König, T. W. Becker, P. Fischer, I. Riemann, and K.-J. Halhuber, "Pulse-length dependence of
40 cellular response to intense near-infrared laser pulses in multiphoton microscopes," *Opt. Lett.*, vol. 24,
41 1190 no. 2, pp. 113–115, 1999.
42 1191
43
44 1192 [129] K. T. Takasaki, J. B. Ding, and B. L. Sabatini, "Live-Cell Superresolution Imaging by Pulsed STED Two-
45 Photon Excitation Microscopy," *Biophys. J.*, vol. 104, no. 4, pp. 770–777, 2013.
46 1193
47
48 1194 [130] P. Bethge, R. Chéreau, E. Avignone, G. Marsicano, and U. V. Nägerl, "Two-Photon Excitation STED
49 Microscopy in Two Colors in Acute Brain Slices," *Biophys. J.*, vol. 104, no. 4, pp. 778–785, 2013.
50 1195
51 1196 [131] E. Schmidt and M. Oheim, "Two-photon imaging induces brain heating and calcium microdomain
52 hyperactivity in cortical astrocytes," *bioRxiv*, 2018.
53 1197
54
55 1198 [132] B. Harke, J. Keller, C. K. Ullal, V. Westphal, A. Schönle, and S. W. Hell, "Resolution scaling in STED
56 microscopy," *Opt. Express*, vol. 16, no. 6, pp. 4154–4162, 2008.
57 1199
58 1200 [133] G. Vicidomini *et al.*, "Sharper low-power STED nanoscopy by time gating," *Nat. Methods*, vol. 8, no. 7,
59 pp. 571–573, 2011.
60 1201

- 1
2
3 1202 [134] Y. Wu and H. Shroff, "Faster, sharper, and deeper: structured illumination microscopy for biological
4 1203 imaging," *Nat. Methods*, vol. 15, no. 12, pp. 1011–1019, 2018.
- 5
6 1204 [135] A. G. York *et al.*, "Resolution doubling in live, multicellular organisms via multifocal structured illumination
7 1205 microscopy," *Nat. Methods*, vol. 9, no. 7, pp. 749–754, 2012.
- 8
9 1206 [136] I. Gregor, M. Spiecker, R. Petrovsky, J. Großhans, R. Ros, and J. Enderlein, "Rapid nonlinear image
10 1207 scanning microscopy," *Nat. Methods*, vol. 14, no. 11, pp. 1087–1089, 2017.
- 11
12 1208 [137] E. N. Ward and R. Pal, "Image scanning microscopy: an overview," *J. Microsc.*, vol. 266, no. 2, pp. 221–
13 1209 228, 2017.
- 14
15 1210 [138] X. Huang *et al.*, "Fast, long-term, super-resolution imaging with Hessian structured illumination
16 1211 microscopy," *Nat. Biotechnol.*, vol. 36, p. 451, Apr. 2018.
- 17
18 1212 [139] E. G. Reynaud, U. Kržič, K. Greger, and E. H. K. Stelzer, "Light sheet-based fluorescence microscopy:
19 1213 More dimensions, more photons, and less photodamage," *HFSP J.*, vol. 2, no. 5, pp. 266–275, Oct. 2008.
- 20
21 1214 [140] E. G. Reynaud, J. Peychl, J. Huisken, and P. Tomancak, "Guide to light-sheet microscopy for
22 1215 adventurous biologists," *Nat. Methods*, vol. 12, no. 1, pp. 30–34, 2014.
- 23
24 1216 [141] R. M. Power and J. Huisken, "A guide to light-sheet fluorescence microscopy for multiscale imaging,"
25 1217 *Nat. Methods*, vol. 14, no. 4, pp. 360–373, 2017.
- 26
27 1218 [142] F. Cella Zanacchi *et al.*, "Live-cell 3D super-resolution imaging in thick biological samples," *Nat. Methods*,
28 1219 vol. 8, no. 12, pp. 1047–1049, 2011.
- 29
30 1220 [143] F. Cella Zanacchi, Z. Lavagnino, M. Faretta, L. Furia, and A. Diaspro, "Light-Sheet Confined Super-
31 1221 Resolution Using Two-Photon Photoactivation," *PLoS One*, vol. 8, no. 7, p. e67667, Jul. 2013.
- 32
33 1222 [144] J. Kim *et al.*, "Oblique-plane single-molecule localization microscopy for tissues and small intact animals,"
34 1223 *Nat. Methods*, vol. 16, no. 9, pp. 853–857, 2019.
- 35
36 1224 [145] P. Hoyer *et al.*, "Breaking the diffraction limit of light-sheet fluorescence microscopy by RESOLFT," *Proc.*
37 1225 *Natl. Acad. Sci.*, vol. 113, no. 13, pp. 3442 LP – 3446, Mar. 2016.
- 38
39 1226 [146] Y. S. Hu *et al.*, "Light-sheet Bayesian microscopy enables deep-cell super-resolution imaging of
40 1227 heterochromatin in live human embryonic stem cells," *Opt. Nanoscopy*, vol. 2, no. 1, p. 7, 2013.
- 41
42 1228 [147] T. A. Planchon *et al.*, "Rapid three-dimensional isotropic imaging of living cells using Bessel beam plane
43 1229 illumination," *Nat. Methods*, vol. 8, no. 5, pp. 417–423, 2011.
- 44
45 1230 [148] L. Gao *et al.*, "Noninvasive Imaging beyond the Diffraction Limit of 3D Dynamics in Thickly Fluorescent
46 1231 Specimens," *Cell*, vol. 151, no. 6, pp. 1370–1385, 2012.
- 47
48 1232 [149] B.-J. Chang, V. D. Perez Meza, and E. H. K. Stelzer, "csiLSFM combines light-sheet fluorescence
49 1233 microscopy and coherent structured illumination for a lateral resolution below 100 nm," *Proc. Natl. Acad.*
50 1234 *Sci.*, vol. 114, no. 19, pp. 4869 LP – 4874, May 2017.
- 51
52 1235 [150] B.-C. Chen *et al.*, "Lattice light-sheet microscopy: Imaging molecules to embryos at high spatiotemporal
53
54
55
56
57
58
59
60

- 1
2
3 1236 resolution," *Science* (80-.), vol. 346, no. 6208, p. 1257998, Oct. 2014.
- 4
5 1237 [151] N. Chakrova, A. S. Canton, C. Danelon, S. Stallinga, and B. Rieger, "Adaptive illumination reduces
6 1238 photobleaching in structured illumination microscopy," *Biomed. Opt. Express*, vol. 7, no. 10, pp. 4263–
7 4274, 2016.
- 8 1239
9
10 1240 [152] J. Dreier *et al.*, "Smart scanning for low-illumination and fast RESOLFT nanoscopy in vivo," *Nat.*
11 1241 *Commun.*, vol. 10, no. 1, p. 556, 2019.
- 12
13 1242 [153] T. Staudt, A. Engler, E. Rittweger, B. Harke, J. Engelhardt, and S. W. Hell, "Far-field optical nanoscopy
14 1243 with reduced number of state transition cycles," *Opt. Express*, vol. 19, no. 6, pp. 5644–5657, 2011.
- 15
16 1244 [154] F. Göttfert *et al.*, "Strong signal increase in STED fluorescence microscopy by imaging regions of
17 1245 subdiffraction extent," *Proc. Natl. Acad. Sci.*, vol. 114, no. 9, pp. 2125 LP – 2130, Feb. 2017.
- 18
19 1246 [155] J. Heine, M. Reuss, B. Harke, E. D'Este, S. J. Sahl, and S. W. Hell, "Adaptive-illumination STED
20 1247 nanoscopy," *Proc. Natl. Acad. Sci.*, vol. 114, no. 37, pp. 9797–9802, 2017.
- 21
22 1248 [156] D. Sage *et al.*, "Super-resolution fight club: assessment of 2D and 3D single-molecule localization
23 1249 microscopy software," *Nat. Methods*, vol. 16, no. 5, pp. 387–395, 2019.
- 24
25 1250 [157] A. Jimenez, K. Friedl, and C. Leterrier, "About samples, giving examples: Optimized Single Molecule
26 1251 Localization Microscopy," *Methods*, 2019.
- 27
28 1252 [158] T. Dertinger, R. Colyer, G. Iyer, S. Weiss, and J. Enderlein, "Fast, background-free, 3D super-resolution
29 1253 optical fluctuation imaging (SOFI)," *Proc. Natl. Acad. Sci.*, vol. 106, no. 52, pp. 22287 LP – 22292, Dec.
30 1254 2009.
- 31
32 1255 [159] S. Geissbuehler *et al.*, "Live-cell multiplane three-dimensional super-resolution optical fluctuation
33 1256 imaging," *Nat. Commun.*, vol. 5, pp. 1–7, 2014.
- 34
35 1257 [160] S. Cox *et al.*, "Bayesian localization microscopy reveals nanoscale podosome dynamics," *Nat. Methods*,
36 1258 vol. 9, no. 2, pp. 195–200, 2012.
- 37
38 1259 [161] N. Gustafsson, S. Culley, G. Ashdown, D. M. Owen, P. M. Pereira, and R. Henriques, "Fast live-cell
39 1260 conventional fluorophore nanoscopy with ImageJ through super-resolution radial fluctuations," *Nat.*
40 1261 *Commun.*, vol. 7, no. 1, p. 12471, 2016.
- 41
42 1262 [162] R. F. Laine *et al.*, "NanoJ: a high-performance open-source super-resolution microscopy toolbox," *J.*
43 1263 *Phys. D. Appl. Phys.*, vol. 52, no. 16, p. 163001, Feb. 2019.
- 44
45 1264 [163] S. Culley, K. L. Tosheva, P. Matos Pereira, and R. Henriques, "SRRF: Universal live-cell super-resolution
46 1265 microscopy," *Int. J. Biochem. Cell Biol.*, vol. 101, pp. 74–79, 2018.
- 47
48 1266 [164] R. J. Marsh *et al.*, "Artifact-free high-density localization microscopy analysis," *Nat. Methods*, vol. 15, no.
49 1267 9, pp. 689–692, 2018.
- 50
51 1268 [165] R. J. Marsh, S. Culley, and A. J. Bain, "Low power super resolution fluorescence microscopy by lifetime
52 1269 modification and image reconstruction," *Opt. Express*, vol. 22, no. 10, pp. 12327–12338, 2014.

- 1
2
3 1270 [166] L. von Chamier, R. F. Laine, and R. Henriques, "Artificial intelligence for microscopy: what you should
4 know," *Biochem. Soc. Trans.*, vol. 47, no. 4, pp. 1029–1040, Jul. 2019.
5 1271
6 1272 [167] C. Belthangady and L. A. Royer, "Applications, promises, and pitfalls of deep learning for fluorescence
7 image reconstruction," *Nat. Methods*, 2019.
8 1273
9 1274 [168] M. Weigert *et al.*, "Content-aware image restoration: pushing the limits of fluorescence microscopy," *Nat.*
10 *Methods*, vol. 15, no. 12, pp. 1090–1097, 2018.
11 1275
12 1276 [169] W. Ouyang, A. Aristov, M. Lelek, X. Hao, and C. Zimmer, "Deep learning massively accelerates super-
13 resolution localization microscopy," *Nat. Biotechnol.*, vol. 36, p. 460, Apr. 2018.
14 1277
15 1278 [170] L. Fang *et al.*, "Deep Learning-Based Point-Scanning Super-Resolution Imaging," *bioRxiv*, 2019.
16 1279 [171] S. Culley *et al.*, "Quantitative mapping and minimization of super-resolution optical imaging artifacts," *Nat.*
17 *Methods*, vol. 15, p. 263, Feb. 2018.
18 1280
19 1281 [172] G. Ball, J. Demmerle, R. Kaufmann, I. Davis, I. M. Dobbie, and L. Schermelleh, "SIMcheck: a Toolbox for
20 Successful Super-resolution Structured Illumination Microscopy," *Sci. Rep.*, vol. 5, p. 15915, Nov. 2015.
21 1282
22 1283
23
24
25
26
27
28
29
30
31
32
33
34
35
36
37
38
39
40
41
42
43
44
45
46
47
48
49
50
51
52
53
54
55
56
57
58
59
60